DISCRETE AND CONTINUOUS
DYNAMICAL SYSTEMS SERIES S

doi:10.3934/dcdss.2021002

DAMPING, STABILIZATION, AND NUMERICAL FILTERING FOR THE MODELING AND THE SIMULATION OF TIME DEPENDENT PDES

Jean-Paul Chehab*

Laboratoire LAMFA (UMR CNRS 7352)
Université de Picardie Jules Verne
33 rue Saint Leu, 80039 Amiens Cédex, France

To the memory of Ezzeddine Zahrouni (1963-2018)

Abstract. We present here different situations in which the filtering of high or low modes is used either for stabilizing semi-implicit numerical schemes when solving nonlinear parabolic equations, or for building adapted damping operators in the case of dispersive equation. We consider numerical filtering provided by mutigrid-like techniques as well as the filtering resulting from operator with monotone symbols. Our approach applies to several discretization techniques and we focus on finite elements and finite differences. Numerical illustrations are given on Cahn-Hilliard, Korteweig-de Vries and Kuramoto-Sivashinsky equations.

1. **Introduction.** One of the particularly hard issues in hydrodynamics is the modeling of damping phenomena: according to the physical situations, viscous (entire or fractional power of $-\Delta$), local or non local additional terms (half-time or half-space derivative) have been proposed to represent the damping and the fitting with real physical data still remains a challenge, we refer the reader, e.g., to [57, 58]. The mathematical analysis of the long time behavior of the solutions of the resulting models is also essential to the understanding of the underlying physics [23, 42, 43, 44, 45, 48]. Of course the derivation of appropriate and robust numerical schemes is crucial to capture the dynamics and also to point out mathematical properties that are difficult to establish, [12, 21, 30, 40]. It is to be noticed that the presence of a damping term can be seen as a stabilization technique used in control theory, see [50, 59].

Let us look now to an apparently different topic: the conception of numerical solvers for nonlinear parabolic equations. It is a classical technique to enhance the stability of semi-implicit time schemes by adding a damping term (e.g. a proper dissipative term) while preserving the consistency of the discretization. Ideally, the stabilizing term must damp hardly the high frequency components (to prevent blowing up oscillations) and slightly the low frequency ones (to preserve the consistency). The additional stabilizing term is nothing else but a damping term and can

2020 *Mathematics Subject Classification.* Primary: 35B40, 35K55, 65M06, 65M55, 65M60.

Key words and phrases. Cahn-Hilliard equation, Korteweig-de Vries equation, Kuramoto-Sivashinski equation, finite differences compact Schemes, finite differences, multigrid methods, stability, numerical filters, damping modelling.

* Corresponding author: Jean-Paul Chehab.

be interpreted as a low-pass filter. This approach necessitates the ability to separate high and low mode components of signal and then to chose or to design the damping/stabilizing operator through its symbol to obtain desired filtering properties. This leads to the usage of two different time schemes, one for each set of components; multi-grid as well as hierarchical-like methods including wavelets have been used in that direction, [13, 53, 54, 55].

We propose here to use relations between damping and stabilization when interpreted as low-pass or high-pass filters, depending on the applications, for deriving new numerical schemes and also for building damping operators: we use damping techniques, on the one hand, to stabilize semi-explicit time scheme and, on the other hand, to build damping operator with proper filtering. To this end, we revisit some topics that have been studied by Ezzeddine Zahrouni and his collaborators, and we include new material and new perspectives.

The article is organized as follows: in Section 2 after recalling briefly the notion of filter, we describe several techniques of separation of the scales that allow to decompose a given signal into a mean and a fluctuant part when considering various discretization techniques. Then, in Section 3, we consider very weak damping models for Korteweg-de-Vries equation in which the damping operator is presented as a high-pass filter. In Section 4, we present a Bi-Grid method in finite elements aimed at stabilizing semi explicit schemes for nonlinear reaction diffusion equations; we interpret this method as a low-pass filter stabilization; an application to 2D Cahn-Hilliard System in finite elements is proposed together with stability results and numerical illustrations. Finally, in Section 5, we propose new perspectives by exchanging the rules deriving directly, on the one hand, a stabilization technique with low pass-filters operators and, on the other hand, we build numerical damping modeling by using Numerical filters of multi-grid type. Korteweg-de Vries and Kuramoto-Sivashinki equations are simulated with these techniques. The numerical computations have been realized using both Matlab ® and FreeFem++ [39].

2. **Filters and separation of the scales.**

2.1. **Filters in the Fourier case.**

When dealing with Fourier-like analysis, one can express a sufficiently regular function u belonging to $\mathbf{H}$, a proper Hilbert space, as the converging sum of linear combinations $(w_k)_{k\geq 1}$ a proper Hilbertian basis of $\mathbf{H}$:

$$u = \sum_{k=1}^{+\infty} \hat{u}_k w_k.$$

A filter operator $\mathcal{F}$ can be defined as function $\phi(.)$ of the frequencies λ_k, $k \geq 1$,

$$\mathcal{F}(u) = \sum_{k\in\mathbb{N}^d} \phi(\lambda_k)\hat{u}_k w_k, \tag{1}$$

where λ_k is the wave number sequence, generally eigenvalues of a bounded operator with compact inverse. In numerous applications, the function ϕ is tuned in order to obtain a given effect. The simplest one is a bandwidth pass consisting in taking small values of $\phi(\lambda_k)$ for $\lambda_k \in [\lambda, \Lambda]$ and this is applied in situations of practical interest (signal processing for sound or image), the effective choice of ϕ being governed by physical considerations.

However, in many practical situations ϕ is not available but can be approached by a piecewise function in the frequency space as $\phi(\lambda) = \sum_{k\in\mathbb{N}^d} a_k \chi_{N^1(k)\leq\lambda\leq N^2(k)}$,

with $\bigcup_{k\in\mathbb{N}}[N^1(k),N^2(k)]=\mathbb{N}$, $N^1(k)<N^2(k)$, $\forall k\geq 1$. The coefficient a_k could be tuned or in some situation computed optimally (e.g. in the least square sense) to fit a desired effect, for instance a given final solution, see Figure (1) hereafter.

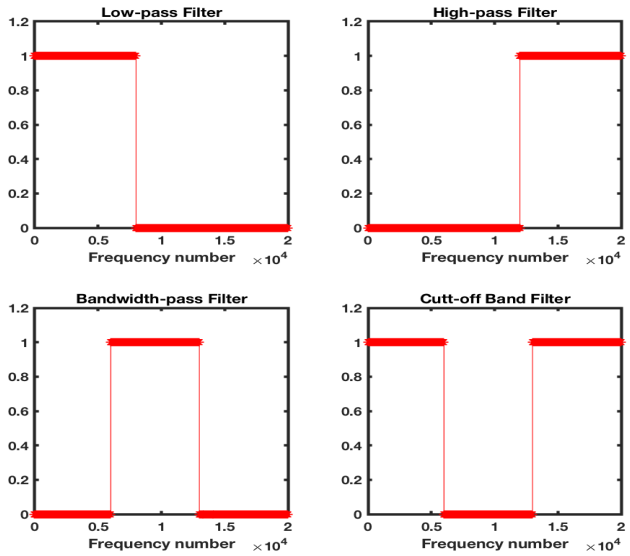

FIGURE 1. Different filters

When dealing with PDEs on bounded domain, it is usual to build the Hilbert basis as normed eigenfunctions of an elliptic operator D:

- $D=-\Delta$ in $\mathbf{H}=\mathbb{H}^1_0(\Omega)$ when considering homogeneous Dirichlet Boundary Conditions
- $D=\alpha Id-\Delta$ in $\mathbf{H}=\mathbb{H}^1(\Omega)$, $\alpha>0$ when considering homogeneous Neumann Boundary Conditions
- $D=-\Delta$ in $\mathbf{H}=\left\{u\in\mathbb{H}^1(\Omega)/\int_\Omega u dx=0\right\}$ when considering periodic or homogeneous Neumann Boundary Conditions

Remark 2.1. Of course, similar filters can be built when using orthogonal polynomials.

We now describe the construction of filters in general situations (spectral as well as non spectral discretization methods).

2.2. **Separation of the scales in spectral case.** When spectral methods (Fourier or not) are used, the separation of the low and of the high frequency components is natural, the signal being expanded in a proper orthogonal basis. Indeed, let $(p_k)_{k\geq 0}$ be a family of (algebraic or trigonometric) polynomials on I, say $\int_I p_k p_\ell \omega dx=0$ when $k\neq\ell$, for a given weight function ω. We obtain both a separation of the scales in space (in the least square sense) and a separation of the frequencies:

- approximation result: $u \simeq \sum_{k=1}^{N} \hat{u}_k p_k$, since p_k is an hilbertian basis of $L^2(I)$, $|I| < +\infty$

$$u_N = \sum_{k=1}^{N} \hat{u}_k p_k \quad = \underbrace{\sum_{k=1}^{N/2} \hat{u}_k p_k}_{Y} \quad + \underbrace{\sum_{k=N/2+1}^{N} \hat{u}_k p_k}_{Z}$$

  For regular u, by the convergence of the serie, for N large enough, we have $\|Z\| \ll \|Y\|$.
- all the roots of p_k are simple and alternates from p_k to p_{k+1}; they belong all in I: as a consequence p_k oscillate more and more in I as $k \to +\infty$ hence the separation in frequencies, as illustrated in Figure (2).

Therefore, Y, the low mode part of u, carries the main part of the energy while the fluctuant part, Z, is a small correction containing the high mode components.

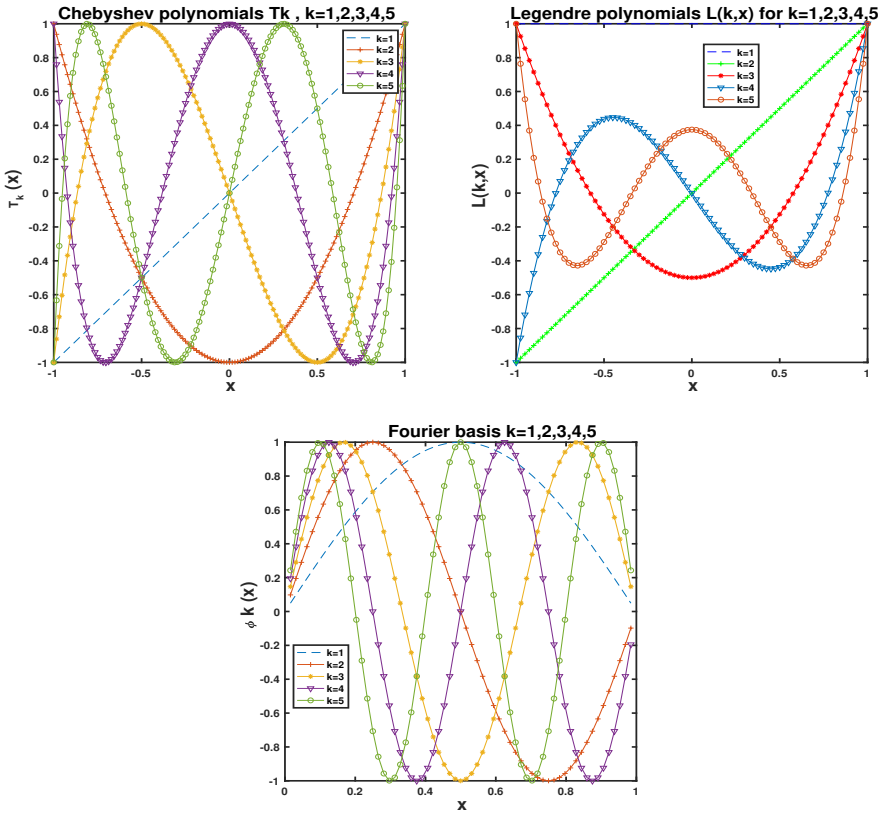

FIGURE 2. Different basis of orthogonal polynomials: Chebyshev polynomials (top left), Legendre polynomials (top right) and Fourier polynomials (bottom)

2.3. **Separation of the scales in hierarchical methods: Finite elements and wavelets.**

2.3.1. *Finite elements.* The generation of the different scales is realized by using hierarchical methods, we refer, e.g., to Bank and Yserentant [4, 66] for a detailed description. Consider an initial (coarse) triangulation T_0 of a polygonal domain Ω: we first build a family of nested triangulations $\{T_0, T_1, ..., T_N\}$ subdivising any triangle of T_k in four congruent triangles leading then to the new triangulation T_{k+1}, see Figure (3) Now, let S_k the finite elements space on the triangulation T_k of Ω

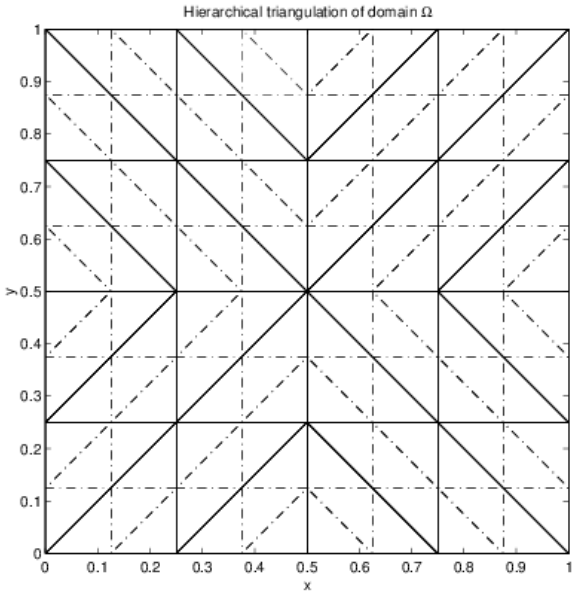

FIGURE 3. Hierarchy of the triangulation of $\Omega =]0,1[^2$: solid line (coarse triangulation), dashed line (complementary triangulation)

and let S_k be the interpolation operator on the nodes of T_k. We define $V_0 = S_0$ and $V_k, k \geq 1$, the subspace of functions that belong in S_k and vanish at the nodes of T_{k-1}. We can decompose in that way a function $u \in S_N$ as

$$u = I_0 u + \sum_{k=1}^{N} (I_k - I_{k-1})\, u.$$

S_N is then the direct sum of $V_0, V_1, ..., V_N$. The hierarchical basis S_N is define as the set of nodal bases of V_k. The quantities Y and Z are defined by

$$Y = I_0 u \qquad \text{et} \qquad Z = \sum_{k=1}^{N} (I_k - I_{k-1})\, u. \tag{2}$$

The Z components are interpolation error, they are associated to small components and also they contain the high frequency components of the solution: by a Shannon-type argument the coarse sparse can only capture the low-frequency components, *a priori* estimates of energy type are given in [4, 66]).

2.3.2. *Wavelets.* When the data is a function (or signal) the wavelet decomposition allows a decomposition in terms of details of different levels, see e.g. [13] for a more detailed practical description of interpolating wavelet and [24] as a monography. We proceed in two steps, similarly to the hierarchical basis in finite elements:

1. Multiresolution Analysis
   Let a $V_j \subset L^2(\mathbb{R})$ a sequence of functional spaces such that:
   - $\overline{\cap V_j} = L^2(\mathbb{R})$ i.e. $\lim_{j\to+\infty} \|f - P_j f\|_2 = 0$ where P_J is the orthogonal projection of f on V_j.
   - there exists a function ϕ (scale function) such that
     $$\phi_{j,k}(x) = 2^{j/2}\phi(2^j x - k)$$
     is a Riesz basis.
2. Wavelet basis (orthonormal case)
   - $\phi_{j,k}$ are an orthonormal basis such that
     $$P_j f = \sum_{k\in\mathbb{Z}} (f, \phi_{j,k})\phi_{j,k}$$
   - We define the *wavelet* ψ by
     $$\psi = \sum_{k\in\mathbb{Z}} \alpha_k \phi(2x - k).$$

   The sequence $\psi_{j,k}$ is an orthonormal basis of $W_j = V_{j+1} \setminus V_j$; we write then
   $$Q_j f = (P_{j+1} - P_j)f = \sum_{k\in\mathbb{Z}}, (f, \psi_{j,k})\psi_{j,k}$$
   so
   $$f = P_0 f + \sum_j \sum_{k\in\mathbb{Z}} (f, \psi_{j,k})\psi_{j,k},$$
   where $(.,.)$ denotes the scalar product in L^2. The coefficients $(f, \psi_{j,k})$ are the details, they represent the fluctuations at the scale j. The term $P_0 f$ is of the order of the physical solution are represent the large eddies, it is also carried by low frequencies.

2.4. **Separation of the scales with a multigrid approach in finite elements.** We consider two levels of discretization (the bi-grid case). As for the Hierarchical finite elements, the two steps to consider to build the separation of the high and the low mode components are based on the use of coarse and fine grids (or spaces) W_H and V_h respectively; h is the meshsize of the triangulation attached to V_h and H is the meshsize of the triangulation attached to W_H. Here again, the high modes can be represented in V_h while only low modes can be captured in W_H.

To extract the high mode part of a function $u_h \in V_h$ assumed to be regular enough, we write u as

$$u_h = \tilde{u}_h + z_h. \tag{3}$$

Here $\tilde{u}_h$ is the mean part of the solution, $z_h = u_h - \tilde{u}_h \in V_h$ represents the fluctuant part which carries the high mode components of the solution $u_h \in V_h$; we will see hereafter that it is not necessary to simulate z_h in the schemes thanks to a low-pass filter balance. As discussed above, this decomposition can be obtained by using several embedded approximation spaces, as in the hierarchical methods but here we

can avoid to build a hierarchical basis. We propose the following procedure: consider V_h (resp. W_H) the fine (resp. the coarse) finite elements space. We introduce the prolongation operator $\mathcal{P} : W_H \to V_h$ by

$$(u_H - \mathcal{P}(u_H), \phi_h) = 0, \forall \phi_h \in V_h. \tag{4}$$

Using the previous notations we write $Y = \tilde{u}_h = \mathcal{P}(u_H)$ and $Z = z_h$.

It is important to note that the embedding $W_H \subset V_h$ is not mandatory and it is a first advantage as respect to hierarchical methods; of course compatibility conditions on W_H and V_h has to be satisfied to insure that the prolongation is uniquely defined. More precisely if we denote by $(\phi_i)_{i=1}^N$ and $(\psi_j)_{j=1}^M$ two bases of V_h and of W_H respectively $(M < N)$, we can define the matrix B_H^h as $(B_H^h)_{i,j} = (\phi_i, \psi_j),\ i = 1, \cdots, N,\quad j = 1, \cdots, M$. The prolongation step can be written as

$$M_h \mathcal{P}(u_H) = B_H^h u_H,$$

where M_h is the mass matrix relative to $(\phi_i)_{i=1}^N$ .Consequently $\mathcal{P}(u_H)$ is uniquely defined whenever the rank of B_H^h is maximal, say $rank(B_H^h) = M$. We represent in Figure (4) resp. the low and the high mode components (resp. Y and Z) attached to the function $u(x, y) = \cos\big(5(1 - x^2 - y^2)\big)$ on the unit disk when using $\mathbb{P}_2$ Finite Elements. We observe that while Y captures accurately the function, Z is a small and oscillating fluctuant part; in Figure (5) we have represented the magnitude of the Fourier coefficients of u and those of Z and we observe that Z is indeed supported by the high components.

To give a ground to the previous description, recall the following results for which we refer to [1] for a detailled presentation.

Proposition 2.2. *Let W_H and V_h be two FEM spaces built on $\mathcal{C}^0$ reference elements. Assume that $\forall u_H \in W_H, ((u_H, \phi_h) = 0, \forall \phi_h \in V_h \Rightarrow u_H = 0)$ Then, B_H^h is injective. Moreover, there exists two constants β and $\alpha_H^h > 0$ such that $0 < \alpha_H^h < \beta \leq 1$ and*

$$\alpha_H^h \|u_H\| \leq \|\mathcal{P}(u_H)\| \leq \beta \|u_H\|, \forall u_H \in W_H. \tag{5}$$

Proposition 2.3. *Let W_H and V_h be two FEM spaces that we assume to be of class $\mathcal{C}^0$ and associated to nested regular triangulations of Ω, a regular bounded open set of $\mathbb{R}^n$; $(K, P, \Sigma)$is the reference element. For $u \in \mathbb{H}^{k+1}(\Omega)$ (the Sobolev space of order $k + 1$), we denote by $u_h = \Pi_h u$ and $u_H = \Pi_H u$ the P-interpolate of u in V_h and W_H respectively. We assume that $\mathbb{P}_k \subset P$. We have the following estimate:*

$$\|u_h - \mathcal{P} u_H\|_{L^2(\Omega)} \leq C H^{k+1} \|u\|_{\mathbb{H}^{k+1}(\Omega)}.$$

An important issue is the concentration of the main computational effort on the coarsest (yet lower dimensional) subspace $W_H \subset V_h$ especially when $\dim(W_H) < \dim(V_h)$.

2.5. **Low-pass filtering in finite differences: A signal processing approach.** For the sake of simplicity consider a problem that we discretize in finite differences on a cartesian periodic domain.

We here give a version of stabilized scheme when using numerical filters; we point out the stabilization effect brought by the presence of these numerical filters in Section 5. In particular the filter will be implemented explicitly in the numerical scheme as an additional explicit (numerical) operator; usually the filtering is used as a post-treatment to stabilize the computations, see e.g. [10].

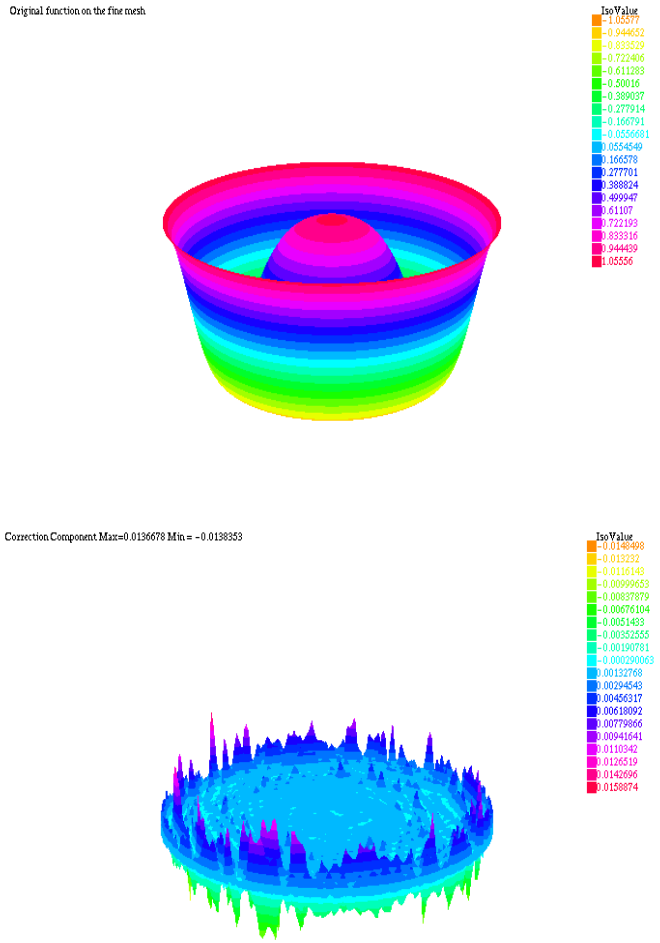

FIGURE 4. 3D output and iso-values for $u(x,y) = \cos\big(5(1-x^2-y^2)\big)$ on the unit disk. The function u with $\mathbb{P}_2$ elements (top) and the z_h components (bottom).

We first consider the 1D case and periodic boundary conditions. We define $2N$ regularly spaced points $x_i = ih, i = 0, \cdots 2N-1$ with $h = \frac{1}{N}$. We start by defining the 2mth order interpolation scheme that associates to every $u(x_i)$ of odd indice $(i = 2p-1)$ a proper mean value of the function u computed with only values of u at odd indices $(u(2i \pm 2p))$, namely

$$u_{2i-2} = \sum_{p=0}^{m-1} a_p \frac{u_{2i-2p-1} + u_{2i+2p+1}}{2}. \tag{6}$$

For a regular function u, we have

$$u(x_{2i}) - \sum_{p=0}^{m-1} a_p \frac{u(x_{2i-2p-1}) + u(x_{2i+2p+1})}{2} = O(h^{2m}). \tag{7}$$

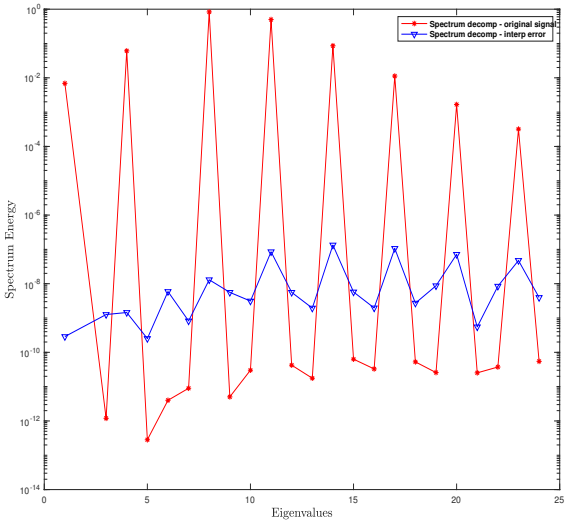

FIGURE 5. Function $u(x,y) = \cos\big(5(1-x^2-y^2)\big)$ on the unit disk. Eigenfunction (Fourier) coefficients on the fine mesh for the original function u_h (red line) and the associated correction z_h (blue line).

At this point, we define the matrix F as

$$\begin{cases} F_{2i-1,2i-1} = 1, & i = 1, \cdots, N, \\ F_{2i,2i-2p-1} = \dfrac{a_p}{2}, & i = 1, \cdots, N, p = 0, \cdots, m, \\ F_{2i,2i+2p+1} = \dfrac{a_p}{2}, & i = 1, \cdots, N, p = 0, \cdots, m. \end{cases}$$

Using Taylor expansion, we find that the coefficients a_p are computed as the solution of the linear system

$$Va = b,$$

with

$$V = \begin{pmatrix} 1 & 1 & 1 & \cdots & 1 \\ 1 & 4 & 9 & \cdots & m^2 \\ & & & & \\ \vdots & & & & \vdots \\ 1 & 2^{2m-2} & & & m^{2m-2} \end{pmatrix} \text{ and } b = \begin{pmatrix} 1 \\ 0 \\ \vdots \\ \vdots \\ 0 \end{pmatrix}.$$

The matrix $G = Id - F \in \mathcal{M}_n(\mathbb{R})$ is a numerical low-pass filter.

At this point we formulate the following remarks:

- first, we used here for simplicity periodic boundary conditions. This technique could be applied in more general situation, e.g. with homogeneous Dirichlet or Neumann boundary conditions using compact interpolation schemes to filter, see Lele [51],

- we here proceed as in multigrid frameworks considering two levels of discretization: given $h = \frac{1}{2n}$, the coarse grid $G_{2h} = \{x_i = 2hi, i = 0, \cdots n-1\}$ and the fine grid $G_h = \{x_i = ih, i = 0, \cdots 2n-1\}$. The filtering consists in computing proper local average of the function u at the grid points of $G_h \subset G_{2h}$ using formula 6 and to leave unchanged the values of u at the grid points of G_{2h}; the resulting vector $\bar{u}$ carries low frequencies components of u the high ones are smoothed by the average procedure ; the resulting signal $z = u - \bar{u}$ is a high modes correction of $\bar{u}$ to u, of small amplitude for u sufficiently regular, the average being computed such that (7) is satisfied.

  When considering periodic boundary conditions, the filtering procedure consists in sampling a function on given regular grid points composed of both coarse grid points (that belong on G_{2h} and that are referred by $\times$) and of complementary grid points (that belong on $G_h \setminus G_{2h}$ and that are referred by o), see hereafter. The signal Fu coincide with u on G_{2h}, and the values on $G_h \setminus G_{2h}$ are replaced by the local average values (6). The fluctuant part of the signal u is $u - Fu$.

$$\times \quad o \quad \times \quad o \quad \times \quad o \quad \times \quad o$$

- It has to be noticed that this procedure can be repeated recursively using nested grids $G_\ell = G_h \subset G_{\ell-1} = G_{2h} \subset ... \subset G_0 = G_{2^\ell h}$; G_0 being the coarsest grid and G_ℓ the finest grid. The filtering (6) is then applied successively between two consecutive grid levels G_j and G_{j-1} as in the bi-grid case defining several level of high modes correction $z_j \in G_j$. This approach led to the Incremental Unknown (IU) method which consists in reorganizing the unknowns in coarse grid values Y and in the sequence of the grid corrections correction z_j $G_j \setminus G_{j-1}$, $j = 1, \cdots, \ell$, and to treat numerically each bloc of components with a different scheme, see [18] and the references therein.

As an illustration, we give hereafter in Figure 6 the decomposition of the signal $u(x) = \sin(2\pi x)+\sin(6\pi x)+\sin(12\pi x)+0.1\sin(20\pi x)+0.1\sin(30\pi x)+0.1\sin(120\pi x)$ into its low and high frequency components when using the numerical filtering. This procedure can be extended to 2D and 3D case when considering cartesian domains. We display hereafter in Figure 7 the symbolic location of coarse grid points ($\times$) and of complementary grid points (o) in 2D when considering various Boundary conditions: periodic, homogeneous Dirichlet and homogeneous Neumann.

2.6. **Separation of the scales and multilevel methods.** The separation of the scale provided, e.g. by one of the techniques described above is lead to build new numerical schemes in which low mode and high modes components of the solution are treated differently. When spectral discretization techniques are used, the decomposition of the solution into low and high mode components is clear and different bandwidth of frequencies can be considered to distinguish several levels of details; this approach has been applied for Burgers and Navier-Stokes equations, we refer to [26, 28, 29] for general presentations. When non spectral discretization are used, the separation sales can be obtained by using hierachical approaches: the transfer matrix associated is used both as a pre-conditioner of the stiffness matrices and also to generate different levels of scales, from the coarsest one associated to the lower frequencies whose the elements are of the order of the physical solution to the finest one whose the elements are built as proper interpolation errors and which contains the high mode components. We refer to the non-exhaustive list

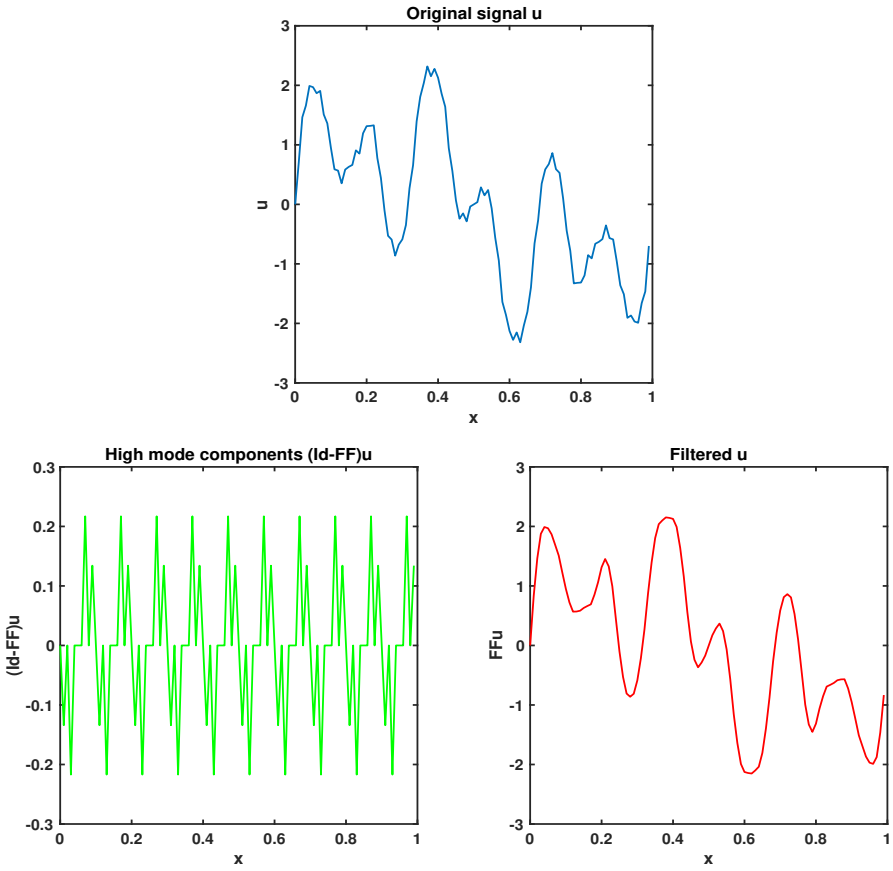

FIGURE 6. Decomposition of the signal $u(x) = \sin(2\pi x) + \sin(6\pi x)+\sin(12\pi x)+0.1\sin(20\pi x)+0.1\sin(30\pi x)+0.1\sin(120\pi x)$, $N = 100, m = 8$. Original signal (top), high frequencies fluctuent part (bottom left) and low frequencies mean part (bottom right)

of references: Hierarchical basis in Finite elements [15, 14, 27, 53, 54, 55, 66], Wavelets and Incremental Unknowns [13, 16, 17, 18, 60] for finite differences or finite volume[3, 38].

3. **Damping modeling for dispersive PDEs by high pass-like filtering.**

3.1. **The asymptotic models and various dampings.** We concentrate on the Korteweg-de-Vries model which is obtained from Euler's equations by selecting a particular physical regime: small amplitude elevation, large wavelength, unidirectional propagation, see [65], it addresses then to low frequency regimes. The long time behavior of dissipative asymptotic models is still an important issue: the capture of damping rates in several norms, the measure of regularization effects, the evidence of complex asymptotic dynamics just to name but a few are important question to consider to understand natural phenomena. Mostly, several of these questions are still open and the numerical simulation is a way to capture some properties, to select pertinent models and to develop strategies.

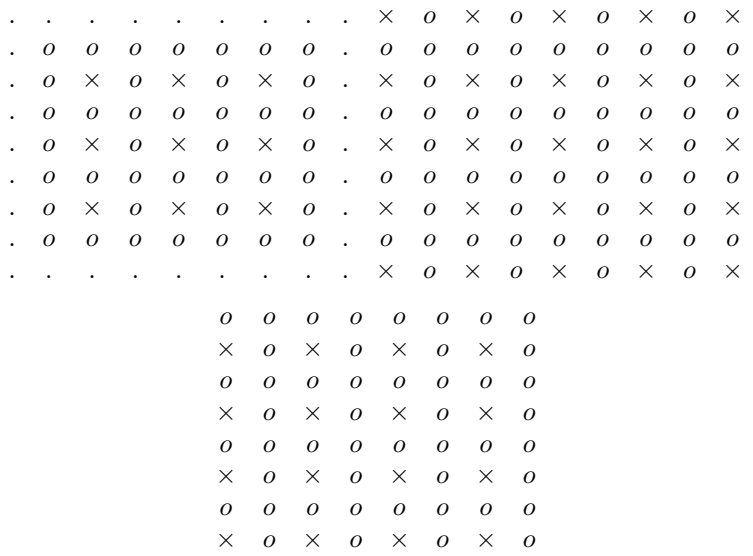

FIGURE 7. Dirichlet BC (Top Left), Neumannn BC (Top Right), Periodic BC (Bottom). The original values are given at grid points $\times$, interpolated values are computed at grid points o. The boundary points are marked by a dot, in the Dirichlet case.

We here focus on KdV equations on the torus $\mathbb{T} = \mathbb{T}(0, L)$; other dispersive models such as BBM (Bona-Benjamin-Mahony) or BO (Benjamin-Ono) equations could also studied following a similar approach, we refer the reader to [40].

Damped Korteweg-de Vries equations appear in different physical situations, they can be expressed in a large generality as

$$u_t + \mathcal{L}(u) + u_{xxx} + uu_x = 0, x \in \mathbb{T},\ t > 0, \tag{8}$$

where $\mathcal{L}$ is a linear operator, defined on a Hilbert space V, subspace of L^2 and satisfying

$$\int_0^L \mathcal{L}(v)v dx \geq 0, \tag{9}$$

for all function $v \in V$, regular enough, in such a way the L^2-norm of the solution is decreasing in time as

$$\frac{1}{2}\frac{d|u|_{L^2}^2}{dt} + \int_0^L \mathcal{L}(u)u dx = 0. \tag{10}$$

We find in the literature different choices for $\mathcal{L}$, depending on the physical situations:

- in their article, [57], Ott and Sudan have proposed a damped KdV equation as a model of Landau damping for ion acoustic wave, the (linear) damping being nonlocal, and in [58] they have presented different models of damping taking $\mathcal{L}(u) = |D|^\alpha u$, where $|D| = \sqrt{-\Delta}$;

- in [33, 32] and in [31] the operators

$$\mathcal{L}(u) = -\nu u_{xx} + \sqrt{\frac{\nu}{2}}\int_0^t \frac{u_x(s)}{\sqrt{t-s}}ds, \tag{11}$$

$$\mathcal{L}(u) = u_x - \nu u_{xx} + \sqrt{\frac{\nu}{2}}\frac{\partial}{\partial t}\int_0^t \frac{u(s)}{\sqrt{t-s}}ds, \tag{12}$$

  have respectively been considered, to model natural damping of water waves, mathematical analysis and simulations can be found also in [12, 23, 30] in which

$$u_t + u_{xxx} + uu_x - \nu u_{xx} - \frac{\sqrt{\nu}}{\sqrt{\pi}}\int_0^t \frac{u_t(s)}{\sqrt{t-s}}ds = 0, \tag{13}$$

  was considered. The mathematical analysis is given in [23] and a numerical study is presented in [30].
- A localized damping in space corresponds to

$$\mathcal{L}(u)(x,t) = \chi_{[a,b]}u,$$

  where $\chi(x)$ is the characteristic function of $[a,b] \subset [0,L]$. This situation have been studied in the context of the stabilization of KdV equations, when the domain is the torus $\mathbb{T}$ [50] or the half line $\mathbb{R}^+$ and $\mathcal{L} = \chi_{[a_0,+\infty[}$ with $a_0 > 0$, [59]; they proved the exponential decay of the solutions in time in proper Sobolev norms; this exponential rate of convergence (after a transient time) is captured numerically in [22].

3.2. **Very weak dampings as high-pass filters.** We begin by defining as we mean by a weak damping operator:

Definition 3.1. L is said to be a weak damping operator for KdV equation

$$u_t + u_{xxx} + L[u] + uu_x = 0,\ x \in \mathbb{T}, t > 0, \tag{14}$$

$$u(x,0) = u_0(x), \tag{15}$$

if there exists $c > 0$ such as

$$0 \leq \int L[u]udx \leq c\|u\|_{L^2}^2 \forall u \in L^2(\mathbb{T}).$$

The case $L = \gamma Id$, with $\gamma > 0$ corresponds to a weak damping model. In this situation we have for sufficiently regular solutions

$$\frac{1}{2}\frac{d\|u\|_{L^2}^2}{dt} + \gamma\|u\|_{L^2}^2 = 0,$$

so the L^2-norm of the solution is exponentially damped in time.

Consider now the forced equations, say

$$u_t + u_{xxx} + L[u] + uu_x = f,\ x \in \mathbb{T}, t > 0 \tag{16}$$

$$u(x,0) = u_0(x) \tag{17}$$

This damping has not a regularizing effect at finite time but, as proved by Ghidaglia [42, 43] and Goubet [44, 45], the regularization arises asymptotically in time. Namely, it allows the equation to posses a finite dimensional attractor which is in a more regular space than the initial data: this is the asymptotic regularization property. Rosa and Cabral presented in [12] numerical evidences of a non trivial long time dynamics for moderate values of γ, time periodic solutions of various cycle length were computed.

A natural question is the following: do we still have the phenomena proven/ pointed out by Ghidaglia, Goubet, Rosa and Cabral for even more weak dampings? At this point we introduce the notion of a *very weak damping*:

Definition 3.2. L is said to be a very weak damping operator for KdV equation

$$u_t + u_{xxx} + L[u] + uu_x = f,\ x \in \mathbb{T}, t > 0, \tag{18}$$

$$u(x,0) = u_0(x), \tag{19}$$

if there exists $c > 0$ such that $(L[u],u)_{L^2} \leq c|u|^2_{L^2}$ and there not exists $d > 0$, such that $(L[u],u)_{L^2} \geq d|u|^2_{L^2}$ for all $u \in \mathcal{D}(L) \cap L^2$, where $\mathcal{D}$ is the domain of L.

A way to build such damping operators was proposed in [21, 22] as follows: given a sequence of strictly positive real numbers $(\gamma_k)_{k\in\mathbb{Z}}$, we define

$$L[u] = L_\gamma(u) = \sum_{k\in\mathbb{Z}} \gamma_k \hat{u}_k e^{\frac{2i\pi kx}{L}}. \tag{20}$$

Of course, if the sequence γ_k is bounded from below, say $\gamma_k \geq \gamma > 0$, the damping is exponential as before, so a special attention is then given to the case:

$$\lim_{k\to+\infty} \gamma_k = 0.$$

The damping is here then weaker than when $\gamma_k = \gamma$ and can be interpreted as a high-pass filter. Indeed

- when considering a steady problem $L_\gamma u$ is a low-pass filter since it damps the high-frequencies: in the ideal filter case, we take $\gamma_k = 1$ for $|k| \leq M$ and $\gamma_k = 0$ for $|k| > M$. Then $L_\gamma u$ selects only the low frequencies of u. We will consider rather the situation $\lim_{k\to+\infty} \gamma_k = 0$, the hypothesis $\gamma_k > 0$ being important to establish the decay in time.
- for the evolutive case (the roles are exchanged): looking on the linear part of the equation

  $$u_t + u_{xxx} + L_\gamma u = 0$$

  we have $\hat{u}_k(t) = e^{(-i(\frac{2\pi k}{L})^3 - \gamma_k)t}\hat{u}_k(0)$ so the low frequencies are much more damped as the high ones since $\lim_{k\to+\infty} \gamma_k = 0$; Figure (8) hereafter illustrates the low-pass filter and its transformation into high-pass filters when taking its negative exponential transformation.

At this point we recall the following results on the decay of the solution in the L^2-norm and we refer the reader to [21] for more details.

Proposition 3.3 (Convergence of the solutions to zero)**.** *We define the energy space* $H\gamma(\mathbb{T}) = \{u \in L^2(\mathbb{T}) / \sum_{k\in\mathbb{Z}} \gamma_k |\widehat{u}_k|^2 < +\infty\}$.

- *Consider the linear homogeneous equation*

  $$u_t + L_\gamma u = 0.$$

  Assume that $\gamma_k > 0, \forall k \in \mathbb{Z}$ *and that* $u_0 \in H^{\beta/\gamma}$. *Then,* $|u|^2_\beta \leqslant \frac{e^{-1}}{2t}|u_0|^2_{\frac{\beta}{\gamma}}$.

  More generally, assume that $\gamma_k \in [0,1], \forall k \in \mathbb{Z}$ *and that* $u_0 \in H_{\frac{1}{\gamma^s}}$.

  Then, for every $s > 0$, $|u|^2_{L^2} \leqslant \min\left(e^{-s}\left(\frac{s}{2t}\right)^s |u_0|^2_{\frac{1}{\gamma^s}}, |u_0|^2_{L^2}\right)$.
- *Consider now the the nonlinear homogeneous equation Assume that* $\bar{u}(0) = 0$ *and* $\gamma_k > 0$ *then*

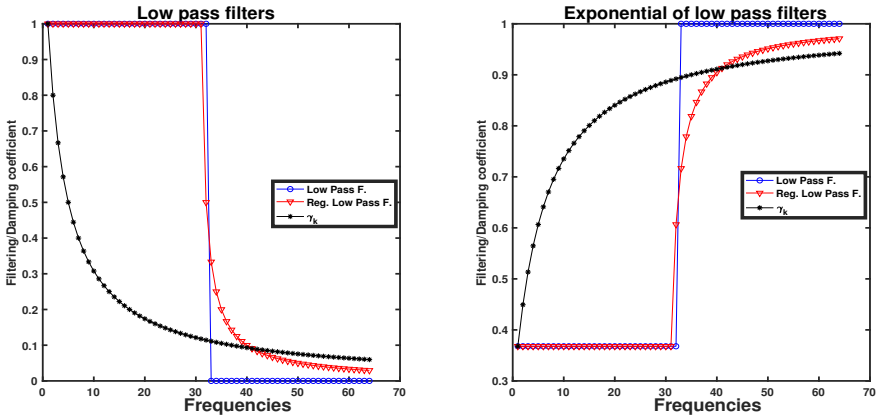

FIGURE 8. Low-pass filters: (left) - Exponential of low pass filters = high-pass filter (right)

i. $\lim_{t\to+\infty} |u|_{L^2} = 0.$

ii. In addition, if $\bar{u}(0) = 0$ *and if* $\exists c > 0$ *such that* $\gamma_k \geq c > 0, \forall k \in \mathbb{Z}$ *then* $|u|_{L^2} \leq \kappa e^{-ct} |u|_L^2$.

Remark 3.4. These results show that when $\gamma_k > 0$, $\lim_{k\to+\infty} \gamma_k = 0$, the orbit converge to 0 in L^2, but it can be at an arbitrary slow rate, it depends on how γ_k converge to 0 as k goes to infinity.

An important issue of the design of very weak damping is the preventing of the blow up in supercritical cases. Consider the Generalized KdV equation (GKdV)

$$u_t + u_{xxx} + u^p u_x = 0, \ x \in \mathbb{T}, t > 0, \tag{21}$$

$$u(x,0) = u_0(x). \tag{22}$$

This equation is known to present finite time blow up solutions when $p \geq 4$, see [5, 7], for particular initial data (called Blowing Up Initial Data or BUID). It is then interesting to try to compute (at least numerically) a very weak operator that, for a given BUID, prevents the blow up. Pierre Garnier in [40] built a very weak damping as a band-width filter using a Fourier discretization in space; the damping is constant per bandwidth ($L_\gamma(u) = \sum_{k\in\mathbb{N}^d} a_k \chi_{N^1(k)\leq|k|\leq N^2(k)} \hat{u}_k e^{\frac{2i\pi kx}{L}}$) and is computed by dichotomy as the lowest possible level (lowest values of $a_k > 0$). The damping depends on the initial data. We recall that a soliton for GKdV is given by

$$\varphi(x,t) = \left(\frac{(p+1)(p+2)(c-1)}{2}\right)^{1/p} \cosh^{-2/p}\left(\pm\sqrt{\frac{(c-1)}{4}}p(x-ct-d)\right).$$

The choice of a initial data for simulating a blow up is commonly a perturbed soliton:

$$u_0(x) = \sigma\varphi(x,0),$$

with $\sigma = 1.01$ or $\sigma = 0.99$ (see [49, 40]).

4. Stabilization techniques for parabolic equations by low pass- like filtering.

4.1. **The different approaches in finite elements.** When considering parabolic equations, it is well known that the stability of a time marching scheme is governed by its capability to contain the propagation of the high frequency components of the solution. Usually the explicit or semi explicit time schemes require les computational effort than the fully explicit ones but they suffers from a hard time step limitation to prevent the instability caused by the expansion of the high mode components. A way to obtain a good compromise between a fast iteration (explicit or semi implicit scheme) and stability (fully implicit schemes) is to add to the first ones a stabilizing term.

$$\frac{u^{(k+1)}-u^{(k)}}{\Delta t}+Au^{(k+1)}+f(u^k)=0, \tag{23}$$

There exist many different stabilization procedures that can be applied to a large variety of schemes used for reaction-diffusion equations, see, e.g. [56, 41, 63], particularly those based on hyperbolic perturbations that we will not consider here.

- parabolic perturbation (first order stabilization)

$$\frac{u^{(k+1)}-u^{(k)}}{\Delta t}+Au^{(k+1)}+\tau(u^{(k+1)}-u^{(k)})+f(u^k)=0, \tag{24}$$

  The stabilization term can be written as $\tau\Delta t\dfrac{u^{(k+1)}-u^{(k)}}{\Delta t}$ and then appears as a first order perturbation which increases the dissipation
- hyperbolic perturbation (second order stabilization)

$$\frac{u^{(k+1)}-u^{(k)}}{\Delta t}+Au^{(k+1)}+\tau(u^{(k+1)}-2u^{(k)}+u^{(k-1)})+f(u^k)=0, \tag{25}$$

  The stabilization term can be written as $\tau(\Delta t^2)\dfrac{u^{(k+1)}-2u^{(k)}+u^{(k-1)}}{(\Delta t)^2}$ and then appears as a second order perturbation which increases the dissipation since the scheme corresponds to the time discretization of a damped nonlinear wave equation:

$$\frac{\partial u}{\partial t}+\tau(\Delta t)^2\frac{\partial^2 u}{\partial t^2}+f(u)=0.$$

  A more accurate scheme can be obtained using a Gear method as

$$\frac{3u^{(k+1)}-4u^{(k)}+u^{(k-1)}}{2\Delta t}+Au^{(k+1)}+\tau(u^{(k+1)}-2u^{(k)}+u^{(k-1)})+f(u^k)=0. \tag{26}$$

4.2. **Low-pass filtering for nonlinear parabolic equations: a bi-grid approach in finite elements.** We here follow. [1, 63]. For the sake of simplicity, consider the finite element approximation to the heat equation by forward Euler's method:

$$(u_h^{k+1},\phi_h)+\Delta t(\nabla u_h^k,\nabla\phi_h) \quad =(u_h^k,\phi_h)+\Delta t\tau(f,\phi_h),\ \forall\phi_h\in V_h. \tag{27}$$

This scheme has a restrictive stability condition due to its weak capability to contains the high frequency components propagation and the addition of a proper damping term is necessary to enhance the stability of the scheme. Following [1, 63],

we propose to add the term $\tau\Delta t(u_h^{k+1}-u_h^k,\phi_h)$, where $\tau>0$ is a stabilizing parameter to be tuned. The new scheme reads as

$$(\frac{u_h^{k+1}-u_h^k}{\Delta t},\phi_h)+\tau(u_h^{k+1}-u_h^k,\phi_h)+(\nabla u_h^k,\nabla\phi_h)=\tau(f,\phi_h),\ \forall\phi_h\in V_h. \quad (28)$$

It can be proved that for $\tau>0$, larger time steps can be taken and for τ large enough values of τ the new scheme is unconditionnally stable. However, an important drawback is that the dynamics of all the components fo the solution are slowed down while only the high mode components need to be damped to enhance the stability, see [1]. A solution is then to damp only the high mode components $z_h^{k+1}-z_h^k$ of $u_h^{k+1}-u_h^k$: they can be computed using two grids as described in Section 2. We find directly

$$z_h^{k+1}-z_h^k=u_h^{k+1}-u_h^k-(\tilde{u}_h^{k+1}-\tilde{u}_h^k).$$

Using the definition of $\tilde{u}_h^k$, it follows that $(\tilde{u}_h^{k+1}-\tilde{u}_h^k,\phi_h)=(u_H^{k+1}-u_H^k,\phi_h)$ and then

$$(z_h^{k+1}-z_h^k,\phi_h)=(u_h^{k+1}-u_h^k-(u_H^{k+1}-u_H^k),\phi_h).$$

It is then non necessary to computed the z components.

Now, and as underlined above, one of the goals of the bi-grid method is to save computational time. To this end the computational effort is concentrated on a coarse finite elements space W_H (of lower dimension) by using implicit and unconditionally time schemes and to simplify the computation of the fine finite elements space V_h (of higher dimension) by using semi-implicit (yet fast) scheme, a gain of CPU time is then expected. The weak stability of the semi-implicit scheme has to be compensated by using a stabilization that we propose to apply only to the high modes components z (of the solution), which are at the origin of the instabilities.

$$\begin{aligned}&(u_h^{k+1},\phi_h)+\Delta t(\nabla u_h^{k+1},\nabla\phi_h)+\Delta t\tau(u_h^{k+1}-u_h^k,\phi_h)\\&=(u_h^k,\phi_h)+\Delta t\tau(u_H^{k+1}-u_H^k,\phi_h),\ \forall\phi_h\in V_h.\end{aligned}$$

This scheme extends naturally to the nonlinear case:

Algorithm 1 Two-grid Stabilized Reaction diffusion equation with correction

u_h^0,u_H^0 given

for $k=0,1,\cdots$ **do**

  Solve $(u_H^{k+1},\psi_H)+\Delta t(\nabla u_H^{k+1},\nabla\psi_H)+\Delta t(f(u_H^{k+1}),\psi_H)$
  $=(u_H^k,\psi_H),\ \forall\psi_H\in W_H$

  Solve $(1+\Delta t\tau)(\delta_h^k,\phi_h)+\Delta t(\nabla\delta_h^{k+1},\nabla\phi_h)=\Delta t\tau(u_H^{k+1}-u_H^k,\phi_h)$
  $-\Delta t(f(u_h^k),\phi_h)\forall\phi_h\in V_h$

  Set $u_h^{k+1}=\delta_h^k+u_h^k$

end for

We now consider an embedded sequence of finite element spaces, from the coarsest $\mathcal{V}_{h_0}$ to the finest $\mathcal{V}_{h_m}$, with

$$\mathcal{V}_{h_0}\subset\mathcal{V}_{h_1}\subset\cdots\subset\mathcal{V}_{h_m}$$

In the present work we will concentrate only to the bi-grid case but we can give hereafter the extension of the stabilized method to the multigrid case.

Algorithm 2 Multi-grid scheme:

for $k = 0, 1, \cdots$ **do**
  Solve in $\mathcal{V}_{h_0}$

$$(\frac{u_{h_0}^{k+1} - u_{h_0}^{k}}{\Delta t}, \psi_{h_0}) + (\nabla u_{h_0}^{k+1}, \nabla, \psi_{h_0}) + (f(u_{h_0}^{k}), \psi_{h_0}) = 0, \forall \psi_{h_0} \in \mathcal{V}_{h_0}$$

  for $j = 1, \cdots m$ **do**
    Solve in $\mathcal{V}_{h_j}$

$$(1 + \tau_j \Delta t)(u_{h_j}^{k+1} - u_{h_j}^{k}, \phi_{h_j}) + \Delta t(\nabla u_{h_j}^{k+1}, \nabla \phi_{h_j})$$
$$-\tau_j \Delta t(u_{h_{j-1}}^{k+1} - u_{h_{j-1}}^{k}, \phi_{h_j}) + \Delta t(f(u_{h_j}^{k}), \phi_{h_j}) = 0, \forall \phi_{h_j} \in \mathcal{V}_{h_j}$$

  end for
end for

4.3. **Application to Cahn-Hilliard equation.**

4.3.1. *The bi-grid scheme.* We consider the Cahn-Hilliard equation

$$\frac{\partial u}{\partial t} + \Delta^2 u - \frac{1}{\epsilon^2}\Delta f(u) = 0, \quad x \in \Omega, t > 0. \tag{29}$$

Here $f(u) = u^3 - u$ is the Landau potential, $F(u) = \frac{1}{4}(u^2 - 1)^2$ its primitive and Δ^2 is the bi-laplacean. This equation is completed with homogeneous Neumann boundary conditions $\frac{\partial u}{\partial n} = 0, \quad \frac{\partial(\Delta u - \frac{1}{\epsilon^2} f(u))}{\partial n} = 0$. Essential properties are

- the conservation of the mass

$$\bar{u} = \int_\Omega u(x,t)dx = \int_\Omega u_0(x)dx, \tag{30}$$

- the decay in time of the energy

$$\frac{\partial E(u)}{\partial t} = -\int_\Omega |\nabla(-\Delta u + \frac{1}{\epsilon^2} f(u))|^2 dx \leq 0, \tag{31}$$

where we have set $E(u) = \frac{1}{2}\int_\Omega |\nabla u|^2 dx + \frac{1}{\epsilon^2}\int_\Omega F(u)dx$. To approximate the weak solution it is classical to first considering the equivalent system

$$\begin{array}{l} \frac{\partial u}{\partial t} - \Delta \mu = 0, \quad x \in \Omega, t > 0, \\ \mu = -\Delta u + \frac{1}{\epsilon^2} f(u), \quad x \in \Omega, t > 0, \end{array} \tag{32}$$

and to the mixed variational framework

$$(\frac{\partial u}{\partial t}, \psi) + (\nabla \mu, \nabla \psi) = 0, \quad \forall \psi \in V, \tag{33}$$

$$(\mu, \phi) = (\nabla u, \nabla \phi) + \frac{1}{\epsilon^2}(f(u), \phi), \quad \forall \phi \in W. \tag{34}$$

First, we define our reference scheme that will be used on the coarse space. It is obtained as follows: the discretization in space is realized by a finite element method, using $\mathbb{P}_1$ or $\mathbb{P}_2$ elements; for the time marching scheme we chose the celebrated Eyre's splitting [36] which is unconditionally stable.

Algorithm 3 One grid scheme (Eyre's splitting):

for $k = 0, 1, \cdots$ **do**
  Solve in $V_H \times W_H$
  $$(\frac{u_H^{k+1} - u_H^k}{\Delta t}, \psi_H) + (\nabla \mu_H^{k+1}, \nabla \psi_H) - (\mu_H^{k+1}, \phi_H) + (\nabla u_H^{k+1}, \nabla \phi_H)$$
  $$+\frac{1}{\epsilon^2}((u_H^{k+1})^3 - u_H^k, \phi_H) = 0, \forall (\psi_H, \phi_H) \in V_H \times W_H$$
end for

We now can derive the associated two-grids stabilized scheme:

Algorithm 4 Bi-grid Stabilized Cahn-Hilliard

u_h^0, u_H^0 given
for $k = 0, 1, \cdots$ **do**
  Solve in $V_H \times W_H$
  $(u_H^{k+1} - u_H^k, \psi_H) + \Delta t(\nabla \mu_H^{k+1}, \nabla \psi_H) = 0, \ \forall \psi_H \in V_H,$
  $(\nabla u_H^{k+1}, \nabla \phi_H) + \frac{1}{\epsilon^2}((u_H^{k+1})^3 - u_H^k), \phi_H) = (\mu_H^{k+1}, \nabla \phi_H), \ \forall \phi_H \in W_H,$
  Solve in $V_h \times W_h$
  $(u_h^{k+1} - u_h^k, \psi_h) + \Delta t(\nabla \mu_h^{k+1}, \nabla \psi_h) = 0, \ \forall \psi_h \in V_h,$
  $(\nabla u_h^{k+1}, \nabla \phi_h) + \tau(u_h^{k+1} - u_h^k, \phi_h) + \frac{1}{\epsilon^2}(f(u_h^k), \phi_h)$
  $= (\mu_h^{k+1}, \phi_h) + \tau(u_H^{k+1} - u_H^k, \phi_h), \ \forall \phi_h \in W_h.$
end for

Before establishing the stability in energy for the scheme 4, we prove the following result:

Proposition 4.1. *Assume that* $(u_H^0, 1) = 0$. *Assume that* $(1, 1) \in V_H \times W_H$. *Then the sequences* (u_H^k, μ_H^k) *generated by algorithm 3 (one-grid scheme) satisfies the properties:*

- $(u_H^k, 1) = 0, \forall k \geq 0,$
- $E(u_H^{k+1}) \leq E(u_H^{k+1}) \ \forall k \geq 0,$
- $\exists C > 0$ *such that* $\sum_{j=0}^{k} \|u_H^{j+1} - u_H^j\|_{L^2(\Omega)}^2 \leq \frac{2}{C} E(u_H^0).$

Proof. Taking $\phi_H = 1$ in algo. 3 we find directly

$$(\frac{u_H^{k+1} - u_H^k}{\Delta t}, 1) = 0, \ \ \forall k \geq 0. \tag{35}$$

The first assertion is obtained by induction, using the hypothesis $(u_H^0, 1) = 0$.

We now establish the energy diminishing for (u_H^k, μ_H^k). We take $\phi_H = \mu_H^{k+1}$ and $\psi_H = u_H^{k+1} - u_H^k$. We obtain

$$\Delta t \|\nabla \mu_H^k\|_{L^2(\Omega)}^2 + (\nabla u_H^{k+1}, \nabla (u_H^{k+1} - u_H^k)) + \frac{1}{\epsilon^2}((u_H^{k+1})^3 - u_H^k, u_H^{k+1} - u_H^k) = 0.$$

Now using parallelogram identity together with the inequality

$$(a^3 - b)(a - b) \geq \frac{(a^2 - 1)^4}{4} - \frac{(b^2 - 1)^4}{4},$$

we find, after the usual simplifications

$$\begin{aligned}&\frac{1}{\epsilon^2}(F(u_H^{k+1})-F(u_H^k),1)+\Delta t\|\nabla\mu_H^{k+1}\|^2_{L^2(\Omega)}\\&+\frac{1}{2}\left(\|\nabla u_H^{k+1}\|^2_{L^2(\Omega)}-\|\nabla u_H^k\|^2_{L^2(\Omega)}+\|\nabla(u_H^{k+1}-u_H^k)\|^2_{L^2(\Omega)}\right)=0.\end{aligned}\tag{36}$$

So

$$\Delta t\|\nabla\mu_H^{k+1}\|^2_{L^2(\Omega)}+\frac{1}{2}\|\nabla(u_H^{k+1}-u_H^k)\|^2_{L^2(\Omega)}+E(u_H^{k+1})=E(u_H^k).\tag{37}$$

The scheme 3 is then unconditionally stable and is also discrete energy diminishing. We now derive bounds: summing all these relations for $j=0,\dots,k$, we obtain

$$\Delta t\sum_{j=0}^{k}\|\nabla\mu_H^{j+1}\|^2_{L^2(\Omega)}+\frac{1}{2}\sum_{j=0}^{k}\|\nabla(u_H^{j+1}-u_H^j)\|^2_{L^2(\Omega)}+E(u_H^{k+1})=E(u_H^0).\tag{38}$$

Now, since (u_H^k) is a null mean value sequence of functions, we can use Poincaré inequality in space $\dot{H}_1(\Omega)=\left\{u\in H^1(\Omega)/\int_\Omega u dx=0\right\}$: there exists $C>0$ such that

$$\|u_H^{j+1}-u_H^j\|^2_{L^2(\Omega)}\le C\|\nabla(u_H^{j+1}-u_H^j)\|^2_{L^2(\Omega)},\forall j=0,\cdots,k.$$

It follows

$$\sum_{j=0}^{k}\|u_H^{j+1}-u_H^j\|^2_{L^2(\Omega)}\le C\sum_{j=0}^{k}\|\nabla(u_H^{j+1}-u_H^j)\|^2_{L^2(\Omega)},\tag{39}$$

then

$$\sum_{j=0}^{k}\|u_H^{j+1}-u_H^j\|^2_{L^2(\Omega)}\le\frac{2}{C}E(u_H^0).\tag{40}$$

□

We now can establish stability results for algorithm 4

Proposition 4.2. *Let $f\in\mathcal{C}^1(\mathbb{R},\mathbb{R})$ and F its primitive. We make the following assumptions:*

- $L=\|f'\|_\infty<+\infty$,
- $F\ge 0$ *on* $\mathbb{R}$,
- $\displaystyle\int_\Omega u_H^0dx=0=\int_\Omega u_h^0dx$.
- $\tau\ge\frac{L}{\epsilon^2}$.

Then, there exists $\kappa>0$ depending only on Ω, $E(u_h^0)$, $E(u_H^0)$ and τ such that

$$E(u_h^{k+1})\le\kappa,\forall k\ge 0.$$

Scheme 4 is then energy stable.

Proof. Let k be fixed. We take $\phi_h=\mu_h^{k+1}$ and $\psi_h=u_h^{k+1}-u_h^k$. We find

$$\begin{aligned}&\Delta t\|\nabla\mu_h^{k+1}\|^2_{L^2(\Omega)}+\frac{1}{2}\left(\|\nabla u_h^{k+1}\|^2_{L^2(\Omega)}-\|\nabla u_h^k\|^2_{L^2(\Omega)}+\|\nabla(u_h^{k+1}-u_h^k)\|^2_{L^2(\Omega)}\right)\\&+\tau\|u_h^{k+1}-u_h^k\|^2_{L^2(\Omega)}+\frac{1}{\epsilon^2}(F(u_H^{k+1})-F(u_H^k),1)\\&+\frac{1}{2\epsilon^2}(f'(\zeta_h)(u_h^{k+1}-u_h^k),(u_h^{k+1}-u_h^k))=\tau(u_H^{k+1}-u_H^k,u_h^{k+1}-u_h^k).\end{aligned}\tag{41}$$

We use Holder then Young's inequalities

$$\begin{aligned}&\Delta t\|\nabla\mu_h^{k+1}\|^2_{L^2(\Omega)}+\frac{1}{2}\|\nabla(u_h^{k+1}-u_h^k)\|^2_{L^2(\Omega)}+\tau\|u_h^{k+1}-u_h^k\|^2_{L^2(\Omega)}\\&+E(u_h^{k+1})-E(u_h^k)\\&\leq\frac{L}{2\epsilon^2}\|u_h^{k+1}-u_h^k\|^2_{L^2(\Omega)}+\frac{\tau}{2}\|u_H^{k+1}-u_H^k\|^2_{L^2(\Omega)}+\frac{\tau}{2}\|u_h^{k+1}-u_h^k\|^2_{L^2(\Omega)}.\end{aligned}$$

Here $L=\|f'\|_\infty$. Letting $\gamma=\frac{1}{2}\left(\tau-\frac{L}{\epsilon^2}\right)\geq 0$ (according to the hypothesis), we infer

$$\begin{aligned}&\Delta t\|\nabla\mu_h^{k+1}\|^2_{L^2(\Omega)}+\frac{1}{2}\|\nabla(u_h^{k+1}-u_h^k)\|^2_{L^2(\Omega)}+\gamma\|u_h^{k+1}-u_h^k\|^2_{L^2(\Omega)}\\&+E(u_h^{k+1})-E(u_h^k)\leq\frac{\tau}{2}\|u_H^{k+1}-u_H^k\|^2_{L^2(\Omega)}.\end{aligned}$$

Finally, summing these relations for $j=0,\dots k$, we have

$$\begin{aligned}&\left(\gamma\sum_{j=0}^k\|u_h^{j+1}-u_h^j\|^2_{L^2(\Omega)}+\Delta t\sum_{j=0}^k\|\nabla\mu_h^{j+1}\|^2_{L^2(\Omega)}+\frac{1}{2}\sum_{j=0}^k\|\nabla(u_h^{j+1}-u_h^j)\|^2_{L^2(\Omega)}\right)\\&+E(u_h^{k+1})\leq E(u_h^0)+\frac{\tau}{2}\textstyle\sum_{j=0}^k\|u_H^{j+1}-u_H^j\|^2_{L^2(\Omega)}.\end{aligned}\tag{42}$$

At this point, we use (40) and obtain

$$E(u_h^{k+1})\leq\kappa,\tag{43}$$

with $\kappa=E(u_h^0)+\frac{\tau}{C}E(u_H^0)$. □

4.3.2. *Numerical illustration.* We first describe the implementation of the fixed point iteration. We compute u_H^{k+1} from u_H^k as follows:

Algorithm 5 Implementation of Eyre's splitting:

1: **Set** $u_H^{k,0}=u_h^k$
2: **for** $m=0,1,\cdots$ **do**
3: **Solve** $(\frac{u_H^{(k,m+1)}-u_H^{(k)}}{\Delta t},\psi_H)+(\nabla u_H^{k,m+1},\nabla\psi_H)$
4: $\qquad+\frac{1}{\epsilon^2}((u_H^{k,m})^2(u_H^{k,m+1})-u_H^k,\psi_H)=0,\forall\psi_H\in W_H.$
5: **end for**
6: **Set** $u_H^{k+1}=u_h^{k,m+1}$

An acceleration of the fixed point is needed for obtaining the convergence without practical restrictions on Δt. To this end we will use Lemaréchal's acceleration. For a better clarity, let us first write Picard's iterates as follows: we denote by $\Phi_k(v_H,u_H^k)$ the application which to u_H^k associates the solution $u_H^*\in W_H$ of the variational problem u_H^*

$$(\frac{u_H^*-u_H^k}{\Delta t},\psi_H)+(\nabla u_H^*,\nabla\psi_H)+\frac{1}{\epsilon^2}((v_H)^2(u_H^*)-u_H^k,\psi_H)=0,\forall\psi_H\in W_H$$

The solution u_H^* is then defined as $u_H^*=\Phi(u_H^*,u_H^{(k)})$. The Picard iterates consist in generating the sequence $v_H^{(m)}\in W_H$ as follows:

$$\begin{aligned}&v^0=u_h^k,\\&\text{for }\ m=0,\dots\\&v_H^{(m+1)}=\Phi(v_H^{(m)},u_H^k).\end{aligned}\tag{44}$$

Unfortunately, in practice, this fixed point method converges only for very small values of Δt. To enhance the stability region, and then to allow to take larger values of Δt, we use the Δ^κ acceleration procedure introduced in [11] and applied in [1, 2, 19] for Allen-Cahn's, weakly damped Schrödinger and BBM equations respectively. In two words, the Δ^κ procedure consists in replacing the Picard iterates by

$$\begin{aligned} &v^0 = u_h^k, \\ &\text{for } \ m = 0, \dots \\ &v^{(m+1)} = v^{(m)} - (-1)^\kappa \alpha_m^\kappa \Delta_\Phi^k v^{(m)}; \end{aligned} \tag{45}$$

where $\Delta_\Phi^\kappa v^{(m)} = \sum_{j=0}^{\kappa} C_j^\kappa (-1)^{\kappa-j} \Phi^{(j)}(v^{(m)}, u^k)$, $C_j^\kappa = \dfrac{\kappa!}{j!(\kappa-j)!}$ is the binomial coefficient and $\Phi^{(j)}$ denotes the j^{th} composition of ϕ with itself. We have

$$\alpha_m^\kappa = (-1)^\kappa \frac{< \Delta_\Phi^1 v^{(m)}, \Delta_\Phi^{\kappa+1} v^{(m)} >}{< \Delta_\Phi^{\kappa+1} v^{(m)}, \Delta_\Phi^{\kappa+1} v^{(m)} >}, \tag{46}$$

where $< .,. >$ denotes the euclidean scalar product in $\mathbb{R}^n$, see [11]. These acceleration procedures have been applied with the Δ^1 (Lemaréchal's method [52] corresponding to $\kappa = 1$).

We show below in Figures (9), (10), (11) respectively the fine and the coarse meshes, the initial and the final solution and the time evolution of the Energy and of the mean value of the solution (which are not affected by the stabilization).

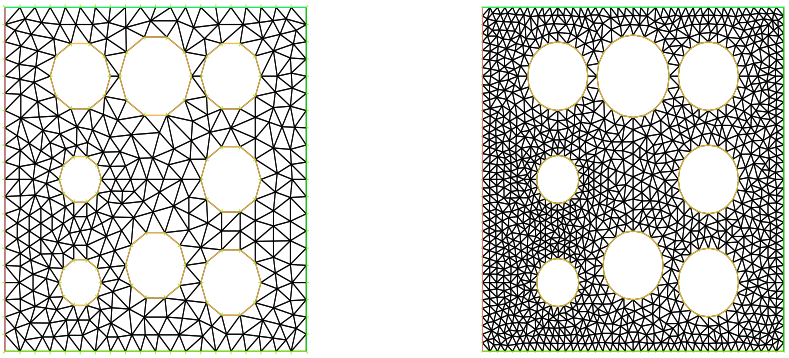

FIGURE 9. Coarse mesh (left) and fine mesh (right)

5. **Exchange of the rules: Stabilization with low pass-filters operators and damping modeling using numerical filters.** We here propose to exchange the rule: in the one hand, use a low-pass filter operator to stabilize explicit and semi-explicit schemes for the solution of parabolic equations and, in the other hand, apply the bi-grid approach to build effective damping models for nonlinear dispersive equations.

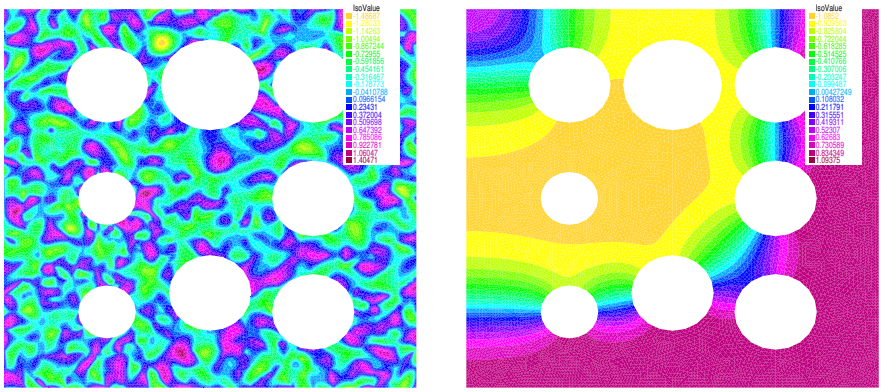

FIGURE 10. Initial solution (left) and Final Solution (right) - $\mathbb{P}_2$ Elements. $\epsilon = 0.08$, $\Delta t = 1.e-4, \tau = 4\epsilon^2, T = 0.012$

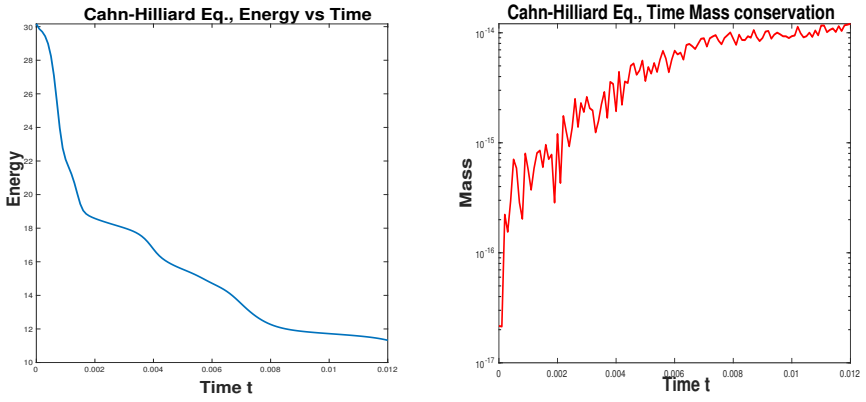

FIGURE 11. Energy (left) and mass (right) vs time - $\mathbb{P}_2$ Elements. $\epsilon = 0.08$, $\Delta t = 1.e-4, \tau = 4\epsilon^2$, $T = 0.012$

5.1. **Damping modeling using numerical filters.** We describe here a method to approach the symbol of a damping operator by a constant-wise function.

Consider the evolution system

$$\frac{\partial u}{\partial t} + \mathcal{A}u + F(u) = 0, \tag{47}$$

which is valid in absence of damping phenomena. We would like to identify a damping operator by fitting a set of experimental data with the enhanced model

$$\frac{\partial u}{\partial t} + \mathcal{A}u + F(u) + \mathcal{B}u = 0, \tag{48}$$

where $\mathcal{B}$ represents the (unknown) damping operator; $\mathcal{B}$ is assumed to be time independent, auto-adjoint and positive definite. When discretizing in space the last

system we get

$$\frac{du}{dt} + Au + F(u) + Bu = 0. \tag{49}$$

Assume that we have at our disposal measured physical data $W(t)$ at discrete times $t_k \in [0, T]$. We would like to compute B in such a way to fit with W. To this end we consider an unconditionally stable time marching scheme, e.g.

$$\frac{w^{k+1} - w^k}{\Delta t} + Aw^{k+1} + F(w^{k+1}) + Bw^{k+1} = 0,$$

with B, a semi definite positive matrix (SDP), to be computed such that the above relation holds for all $0 \leq k\Delta t \leq T = N\Delta t$, the sequence $(w^k)_{k=0}^N$ generated by this scheme depends on B. The matrix B that fits optimally the data is given as the solution of an inverse problem in the least square sense:

$$B_{opt} = \underset{B\ SDP}{\text{Arg min}} \sum_{k=0}^{N} \|w^k - W(k\Delta t)\|^2.$$

Of course, this approach suffers from very important drawbacks: firstly, it needs to recompute totally matrix B when changing the discretization space and, secondly, it is rather hard to interpret the computed matrix B_{opt} in terms of operators. As a simple illustration consider the linear case ($F(.) = 0$). The sequence w^k is supposed to be known as well as the matrix A. We have formally the relations

$$Bw^{k+1} = -\left(\frac{w^{k+1} - w^k}{\Delta t} + Aw^{k+1}\right) = R^{k+1},$$

so

$$Bw^{k+1}(w^{k+1})^T = R^{k+1}(w^{k+1})^T.$$

Summing these relations we get

$$B\sum_{k=1}^{m} w^{k+1}(w^{k+1})^T = \sum_{k=1}^{m} R^{k+1}(w^{k+1})^T.$$

Consequently, a necessary and sufficient condition for computing B uniquely is that the matrix $T_m = \sum_{k=1}^{m} w^{k+1}(w^{k+1})^T$ is full rank, implying to take $m \geq n$. The practical computation of B can be tricky (B is often ill-conditioned) and expansive in CPU time. Finally, all the computations have to be repeated when changing the discretization, e.g., the number of degree of freedom.

For these reasons, we propose a way to approach the symbol of $\mathcal{B}$ by fitting a diagonal ansatz of $\mathcal{B}$ on frequency band-width: the symbol of $\mathcal{B}$ is intrinsic to the operator and do not depend on the chosen discretization. A way to achieve this strategy is to use a multi-grid approach based on embedded approximation spaces, from the coarsest one to the finest one. We present hereafter the feasibility of the approach considering a given two band-witdth damping operator.

5.2. **Filters with bi-grid scheme in finite elements.** A simple bandwidth filtering can be implemented as follows: let τ_1 and τ_2, two strictly positive constants, τ_1 is the damping parameter attached to the low modes and τ_2 is the damping parameter attached to the high ones.

Algorithm 6 Bi-grid scheme: simplified implementation of Scheme 4.1

for $k = 0, 1, \cdots$ **do**
  Solve in W_H
$(\frac{u_H^{k+1} - u_H^k}{\Delta t}, \psi_H) + \tau_0(u_H^{k+1}, \psi_H) + (\nabla u_H^{k+1}, \nabla \psi_H) + (f(u_H^k), \psi_H) = 0, \forall \psi_H \in W_H$
  Solve in V_h

$$(u_h^{k+1} - u_h^k, \phi_h) + \tau_0 \Delta t(u_h^{k+1}, \phi_h) + \Delta t(\nabla u_h^{k+1}, \nabla \phi_h)$$
$$-\tau_0 \Delta t(u_H^{k+1}, \phi_h) + \Delta t(f(u_h^k), \phi_h) = 0, \forall \phi_h \in V_h$$

end for

More generally, we can consider an embedded sequence of finite element spaces, from the coarsest $\mathcal{V}_{h_0}$ to the finest $\mathcal{V}_{h_m}$, with

$$\mathcal{V}_{h_0} \subset \mathcal{V}_{h_1} \subset \cdots \subset \mathcal{V}_{h_m}.$$

We derive the scheme:

Algorithm 7 Multi-grid scheme:

for $k = 0, 1, \cdots$ **do**
  Solve in $\mathcal{V}_{h_0}$
$(\frac{u_{h_0}^{k+1} - u_{h_0}^k}{\Delta t}, \psi_{h_0}) + \tau_0(u_{h_0}^{k+1}, \psi_{h_0}) + (\nabla u_{h_0}^{k+1}, \nabla \psi_{h_0}) + (f(u_{h_0}^k), \psi_{h_0}) = 0,$
$\forall \psi_{h_0} \in \mathcal{V}_{h_0}$
  for $j = 1, \cdots m$ **do**
    Solve in $\mathcal{V}_{h_m}$

$$(u_{h_j}^{k+1} - u_{h_j}^k, \phi_{h_j}) + \tau_j \Delta t(u_{h_j}^{k+1}, \phi_{h_j}) + \Delta t(\nabla u_{h_j}^{k+1}, \nabla \phi_{h_j})$$
$$-\tau_j \Delta t(u_{h_{j-1}}^{k+1}, \phi_{h_j}) + \Delta t(f(u_{h_j}^k), \phi_{h_j}) = 0, \forall \phi_{h_j} \in \mathcal{V}_{h_j}$$

  end for
end for

5.3. **Modelling with piecewise filter damping.**

5.3.1. *A toy model.* We want to mimmic the effect of the damping operator $\mathcal{L}_\gamma$ used in very weak damped KdV Equation: $\mathcal{L}_\gamma u = \sum_{k \in \mathbb{Z}} \gamma_k \hat{u}_k w_k$. Consider the ODE

$$\frac{du}{dt} + \mathcal{L}_\gamma u = 0.$$

For simplicity assume that $\gamma_k = \begin{cases} \tau_0, |k| \le N_1 \\ \tau_1, |k| > N_1 \end{cases}$ τ_0 is the damping parameter attached to the low modes and τ_1 is the damping parameter attached to the high ones. Decompose $u_h = \tilde{u}_h + z_h$.

We introduce the method using Euler time marching scheme. The damping of the law mode components is first computed on the coarse space W_h as

$$(\frac{u_H^{k+1} - u_H^k}{\Delta t}, \psi_H) + \tau_0(u_H^{k+1}, \psi_H) = 0, \forall \psi_H \in W_H$$

then $(\tilde{u}_h - u_H^{k+1}, \phi_h) = 0,\ \forall \phi_h \in V_h$.

The high modes z_h components are damped in V_h with rate τ_1

$$(\frac{z_h^{k+1} - z_h^k}{\Delta t}, \phi_h) + \tau_1 (z_h^{k+1}, \Phi_h) = 0, \forall \phi_h \in V_h,$$

while the low mode $\tilde{u}_h$ on V_h are damped with rate τ_0 as

$$(\frac{\tilde{u}_h^{k+1} - \tilde{u}_h^k}{\Delta t}, \phi_h) + \tau_0 (\tilde{u}_h^{k+1}, \phi_h) = 0, \forall \phi_h \in V_h.$$

Summing these two relations, we obtain (after using the relations "$u_h = \tilde{u}_h + z_h$" and $(\tilde{u}_h - u_H^{k+1}, \phi_h) = 0,\ \forall \phi_h \in V_h$)

$$(\frac{u_h^{k+1} - \tilde{u}_h^k}{\Delta t}, \phi_h) + \tau_1 (u_h^{k+1}, \phi_h) = (\tau_1 - \tau_0)(u_H^{k+1}, \phi_h), \forall \phi_h \in V_h,$$

We give hereafter in Figure (12) a simple illustration of the toy model dynamics for $(\tau_0, \tau_1) = (10, 100)$ and $(\tau_0, \tau_1) = (100, 10)$. We observe the damping is indeed at different rates for the high mode components and for the low ones. The above

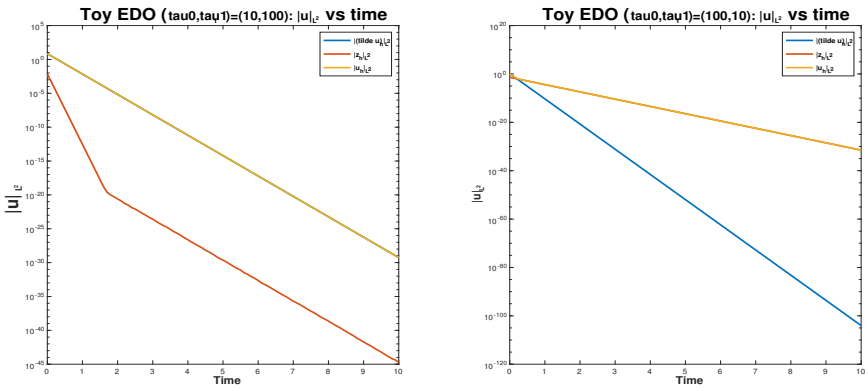

FIGURE 12. $\|u\|_{L^2}$ vs time with $u_0 = \cos(2\pi x/L) + \cos(6\pi x/L) + \cos(12\pi x/L) + \cos(20\pi x/L)$, $(\tau_0, \tau_1) = (10, 100)$ (left) $(\tau_0, \tau_1) = (100, 10)$ (right), $\Delta t = 1.e-1$, $T = 10$, $L = 100$

scheme can be extended in a more general situation in the nonlinear case: consider the equation

$$\frac{du}{dt} + \mathcal{L}_\gamma u + f(u) = 0.$$

The derivation of the bi-grid scheme is similar as above. First, we write the scheme on W_H

$$(\frac{u_H^{k+1} - u_H^k}{\Delta t}, \psi_H) + \tau_0 (u_H^{k+1}, \psi_H) + (f(u_H^{k+1}), \psi_H) = 0, \forall \psi_H \in W_H.$$

$\tilde{u}_h^{k+1}$ is defined as $(\tilde{u}_h^{k+1} - u_H^{k+1}, \phi_h) = 0,\ \forall \phi_h \in V_h$.

Now, we write both the equation satisfied by the z_h and the $\tilde{u}_h$ components:

First, the high modes z_h components are damped in V_h with rate τ_1

$$(\frac{z_h^{k+1}-z_h^k}{\Delta t},\phi_h)+\tau_1(z_h^{k+1},\phi_h)+(f(u_h^k)-\tilde{f}(u_h^k),\phi_h)=0,\forall\phi_h\in V_h,$$

while the low mode $\tilde{u}_h$ on V_h are damped with rate τ_0 as

$$(\frac{\tilde{u}_h^{k+1}-\tilde{u}_h^k}{\Delta t},\phi_h)+\tau_0(\tilde{u}_h^{k+1},\phi_h)+(\tilde{f}(u_h^k),\phi_h)=0,\forall\phi_h\in V_h,$$

By summing these two relations, we obtain

$$(\frac{u_h^{k+1}-\tilde{u}_h^k}{\Delta t},\phi_h)+\tau_1(u_h^{k+1},\phi_h)+(f(u_h^k),\phi_h)=(\tau_1-\tau_0)(u_H^{k+1},\phi_h),\forall\phi_h\in V_h.$$

5.3.2. *Application to KdV equation.* We consider here the periodic KdV equation on $\mathbb{T}(0,L)$

$$u_t+u_{xxx}+uu_x=0,\ x\in\mathbb{T},t>0, \tag{50}$$
$$u(x,0)=u_0(x). \tag{51}$$

This equation possesses the soliton

$$\varphi(x,t)=\frac{A}{\cosh^2(\frac{\kappa}{2}((x-x_0-ct)))},$$

with $A=0.8,\kappa=\sqrt{\frac{A}{3}}$, $c=\kappa^2$ and $x_0=\frac{L}{2}$. The initial data for simulating is then $u_0(x)=\varphi(x,0)$.

To apply the damping technique presented above for the toy problem, we will use finite elements for the space discretization together with a Sanz-Serna scheme for the time marching . We obtain the system

Algorithm 8 KdV System

1: **for** $k=0,1,\cdots$ **do**
2: **Find** $(u_h^{(k+1)},v_h^{(k+1)})\in V_h\times V_h$

$$(\frac{u_h^{k+1}-u_h^k}{\Delta t},\phi_h)-(\partial_x\frac{v_h^{(k+1)}+v_h^{(k)}}{2},\partial_x\phi_h)+\frac{1}{2}(\partial_x(\frac{u_h^{(k+1)}+u_h^{(k)}}{2})^2,\phi_h)$$
$$+(\partial_x u_h^{(k+1)},\psi_h)-(v_h^{(k+1)},\psi_h)=0,\ \forall(\phi_h,\psi_h)\in V_h\times V_h$$

3: **end for**

The presentation of the scheme as a system allows to use $\mathbb{P}_1$ finite elements. We can now apply the bi-grid filter approach described above to obtain a damped system, with different dampings for the low and the high frequency components:

Algorithm 9 Bi-grid scheme damped KdV equation

for $k = 0, 1, \cdots$ **do**

Find $(u_H^{(k+1)}, w_H^{(k+1)}) \in W_H \times W_H$

$$(\frac{u_H^{k+1} - u_H^k}{\Delta t}, \phi_H) - (\partial_x \frac{v_H^{(k+1)} + v_H^{(k)}}{2}, \partial_x \phi_H) + \frac{1}{2}(\partial_x (\frac{u_H^{(k+1)} + u_H^{(k)}}{2})^2, \phi_H)$$

$$+\tau_0 (\frac{u_H^{(k+1)} + u_H^{(k)}}{2}, \phi_H) + (\partial_x u_H^{(k+1)}, \psi_h) - (v_H^{(k+1)}, \psi_H) = 0,$$

$$\forall (\phi_H, \psi_H) \in W_H \times W_H$$

Find $(u_h^{(k+1)}, v_h^{(k+1)}) \in V_h \times V_h$

$$(\frac{u_h^{k+1} - u_h^k}{\Delta t}, \phi_h) - (\partial_x \frac{v_h^{(k+1)} + v_h^{(k)}}{2}, \partial_x \phi_h) + \frac{1}{2}(\partial_x (\frac{u_h^{(k)} + \tilde{u}_h^{(k+1)}}{2})^2, \phi_h)$$

$$+\tau_1 (\frac{u_h^{(k+1)} + u_h^{(k)}}{2}, \phi_h) - \tau_1 (\frac{u_H^{(k+1)} + u_H^{(k)}}{2}, \phi_h) + \tau_0 (\frac{u_H^{(k+1)} + u_H^{(k)}}{2}, \phi_h)$$

$$+(\partial_x u_h^{(k+1)}, \psi_h) - (v_h^{(k+1)}, \psi_h) = 0, \ \forall (\phi_h, \psi_h) \in V_h \times V_h$$

end for

As a simple illustration, we consider the two following situations to underline the low mode regime of the KdV model representing the time evolution of the two first invariants the L^2 norm and the mean value:

- We take $(\tau_0, \tau_1) = (0, 0)$: the KdV equation is not damped and both the mean value and the L^2-norm of the solution are conserved, see Figure 13
- We take $(\tau_0, \tau_1) = (0, 100)$: only the high mode components are damped. Since the KdV model is derived as a low mode approximation, there is almost not damping, see Figure 14
- We take $(\tau_0, \tau_1) = (100, 1)$: the low mode are hardly damped as respect to the high ones. Figure 15

In all cases, the observations agree with those of [21] in Fourier case.

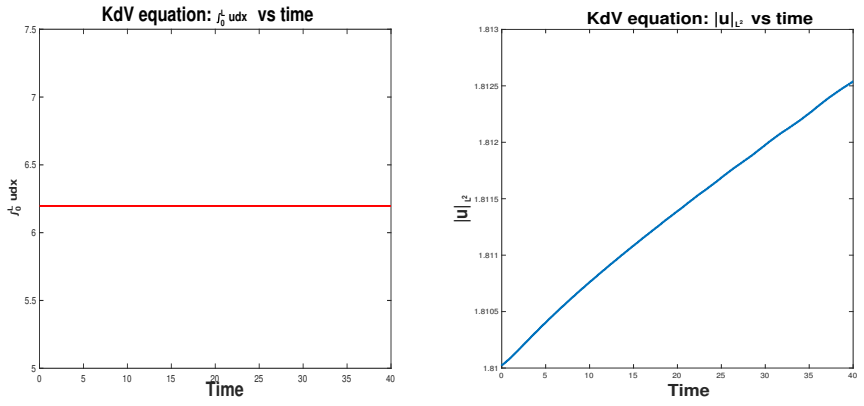

FIGURE 13. KdV $(\tau_0, \tau_1) = (0, 0)$, $\mathbb{P}_1$ Elements. $\Delta t = 1.e-2$, $T = 40$. Mass $\int_0^L u dx$ (left) and L^2-norm $|u|_{L^2}$ (right) vs time

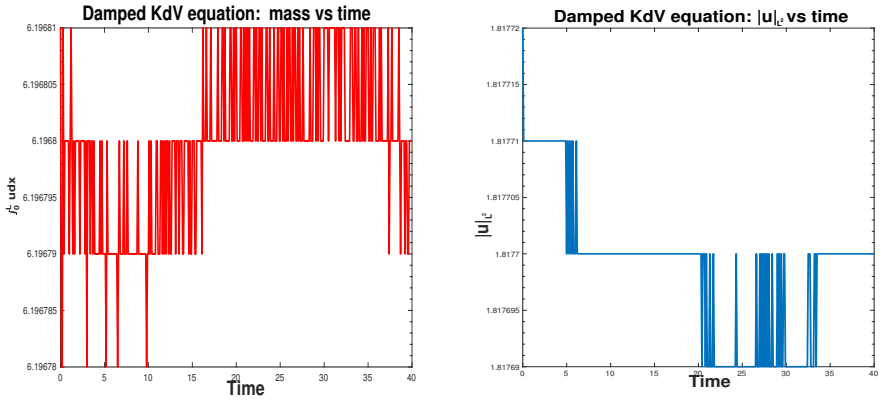

FIGURE 14. KdV $(\tau_0, \tau_1) = (0, 100)$ Low pass damping, $\mathbb{P}_1$ Elements. $\Delta t = 1.e-2$, $T = 40$. Mass $\int_0^L u dx$ (left) and L^2-norm $|u|_{L^2}$ (right) vs time

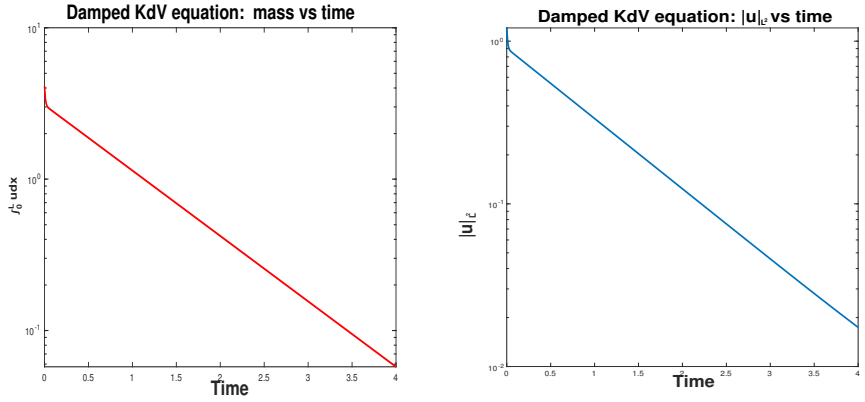

FIGURE 15. KdV $(\tau_0, \tau_1) = (0, 100)$ Low pass damping, $\mathbb{P}_1$ Elements. $\Delta t = 1.e-2$, $T = 4$. Mass $\int_0^L u dx$ (left) and L^2-norm $|u|_{L^2}$ (right) vs time

5.4. **Stabilization with low pass-filters operators : A signal processing low-pass filtering for parabolic equations.** We here use the separation of the scale provided by the numerical filtering presented in Section 2.5.

The matrix $G = Id - F \in \mathcal{M}_n(\mathbb{R})$ is a numerical high-pass filter. Therefore, the damping of the high frequency components can be obtained from scheme (24) as

$$\frac{U^{(k+1)} - U^{(k)}}{\Delta t} + \tau G(U^{(k+1)} - U^{(k)}) + AU^{(k)} = f. \tag{52}$$

5.4.1. *Stabilized schemes.* At this point, we can propose the following explicit stabilized scheme

Algorithm 10 : Explicit-Stabilized with Numerical filtering

for $k = 0, 1, \cdots$ **do**
  Solve $(Id + \tau \Delta t G)\delta^{(k)} = \Delta t(f - Au^{(k)})$
  Set $u^{(k+1)} = u^{(k)} + \delta^{(k)}$
end for

We can give now the "good" generic properties to be satisfied by G

- Damping :$< Gu, u > \geq 0,\ \forall u \in \mathbb{R}^n$
- High-Mode components approximation: let $u \in \mathcal{C}^{2p+2}$, we let $u_i = u(x_i), i = 1, \cdots n$, $u = (u_1, \cdots, u_n)^T$.
  - $\exists C > 0$ independent on u and h such that $\|G\| \leq Ch^{2p}\|u\|$
  - if u is high mode supported $\|Gu - u\|$ is "small"

We will discuss on that aspect elsewhere and concentrate in the present work on numerical evidences.

As a simple illustration, consider the numerical solution of the Heat equation by Algorithm 11. To appreciate the stabilization brought by the high mode damping, we compare both the stability region and the evolution of the error (in L^∞-norm) for the scheme 52 when

- $G = 0$ which gives the Forward Euler's scheme
- $G = A$ which gives the Backward Euler's scheme
- $G = Id$ which gives the globally stabilized Forward Euler's scheme
- $G = Id - F$ which gives the high frequency stabilized Forward Euler's scheme, say Algorithm 11

We also compare the results with the second order stabilized scheme (hyperbolic stabilization 25 together with High frequency filtering):

$$\frac{u^{(k+1)} - u^{(k)}}{\Delta t} + Au^{(k+1)} + \tau G(u^{(k+1)} - 2u^{(k)} + u^{(k-1)}) = f(k\Delta t). \tag{53}$$

We simulate the exact solution $u(x,t) = (\sin(2\pi x) + 0.1\sin(4\pi x) + 0.1\sin(10\pi x) + 0.1\sin(16\pi x))\exp(\sin(t))$; the parameters are $n = 100, m = 4, \Delta t = 9.95\,10^{-5}, \tau = 1.6, 10^4$ First of all we remark that the stability region of the Backward Euler scheme is enhanced thanks to the the stabilization procedure: indeed while the times step limitation of the fully explicit scheme is

$$0 < \Delta t < \frac{2}{\rho(A)} = 5.\,10^{-5},$$

we can choose a nearly double time step for the stabilized schemes: $\Delta t = 9.95\,10^{-5}$. We report hereafter in Figure (16) the time evolution of the error for the schemes Backward Euler's, First order high frequency stabilized, second order stabilized and fully stabilized. We remark that the error of the fully stabilized scheme is important while the curves corresponding to the three other schemes are superposed at a satisfactory level.

As a second illustration, we consider the Kuramoto-Sivashinsky equation (KSE) which describes the propagation of a flam front in some physical situations. We

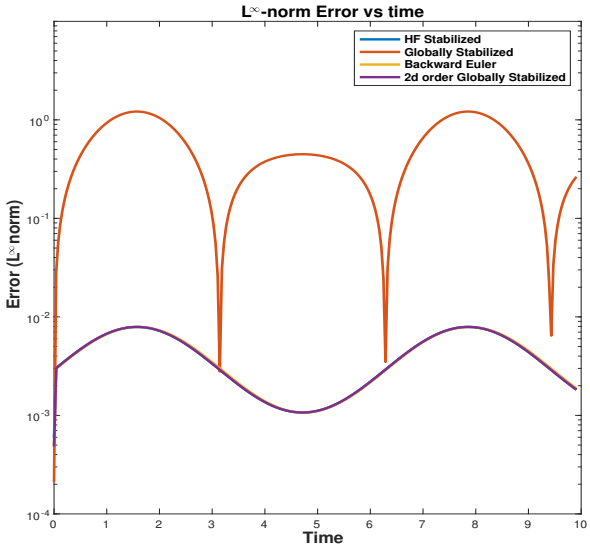

FIGURE 16. Heat Equation - L^∞-norm of the error vs time - $n = 100, m = 4, \Delta t = 9.95\,10^{-5}, \tau = 1.6, 10^4$

consider this equation on the torus $\mathbb{T} = [0, L]$:

$$u_t + u_{xxxx} + u_{xx} + \frac{1}{2}(u_x)^2 = 0, \qquad x \in]0, L[, \qquad t > 0, \tag{54}$$

$$u(0, x) = u_0(x), \qquad x \in]0, L[, \tag{55}$$

$$\frac{\partial^j u}{\partial x^j}(t, x + L) = \frac{\partial^j u}{\partial x^j}(t, x), \quad j = 0, \ldots, 3. \tag{56}$$

The terms u_{xxxx} and u_{xx} are in competition, their sum brings a global dissipation when all the eigenvalues of ∂_{xxxx} dominate those of $-\partial_{xx}$, say when $\frac{2\pi}{L} \geq 1$ or equivalently $L \leq 2\pi$; for larger values of L, a finite and consecutive number of eigenvalues of $\partial_{xxxx} + \partial_{xx}$ are strictly negative; L appears as a bifurcation parameter and for large values, chaotic dynamics is observed, we refer to [47, 64, 67]. We now consider the numerical simulations using as above finite differences for the space discretization: the differential operators are discretized high order compact schemes [51]. We will denote by A_{2j} the discretization matrix of $\partial_{xxxx} + \partial_{xx}$ by a scheme of order $2j$. We now consider the following semi-explicit three schemes:

Algorithm 11 : Explicit-Stabilized schemes for KSE

1: **for** $k = 0, 1, \cdots$ **do**
2: **Solve** $(Id + \tau \Delta t M)\delta^{(k)} = -\Delta t(f(u^k) + A_{2j}u^{(k)})$
3: **Set** $u^{(k+1)} = u^{(k)} + \delta^{(k)}$
4: **end for**

The pratical choices for matrix M are the following:

- $M = A_{2j}$ which gives the Backward Euler's semi-implicite scheme or the classical IMEX scheme

- $M = \tau(Id - F) + A_2$ which gives high frequency (HF) stabilized Forward Euler's scheme

An additional HF stabilized scheme extending the second order stabilization one will be also used:

$$\frac{u^{(k+1)} - u^{(k)}}{\Delta t} + \tau(Id - F)\left(u^{(k+1)} - 2u^{(k)} + u^{(k-1)}\right) + A_2(u^{(k+1)} - u^{(k)})$$

$$= -f(u^k) - A_{2j}u^{(k)}.$$

In the implicit linear part, we use A_2 (which is a sparse matrix) instead of A_{2j} (which is dense once $j \geq 2$) to accelerate the resolution at each time step, as also proposed in [8, 9] for Navier-Stokes and phase fields equations. We did not reported the results for the global stabilized algorithm applied to KSE (corresponding to $M = \tau Id + A_2$) because the dynamics is frozen by the stabilization.

We give hereafter in Figures (17) and (18) the computed KSE solution at final time $T = 140$ (both low and high mode components) together with the time evolution of the mean value, 6th order compact schemes are used. The results agree with those of [13, 67].

6. **Conclusion and perspectives.** The decomposition of numerical approximations of solutions of dissipative or dispersive PDEs into low modes and high modes components can be simply done in various situations (Spectral, Finite Elements, Finite Differences as presented in Section 2; it allows to develop new numerical schemes (using high mode stabilization) but also to design new damping models. As a possible perspectives, we propose to study and implement the multi-grid versions of both stabilized times schemes (algorithm 4) and damped (algorithms 9) with a band width approach. In the particular context of the modeling of the damping of hydrodynamic equations (but not only) the building of a damping operator *via* a band-pass approximation of its symbol using a multi-grid approach seems an interesting option. Damping parameter could be computed optimally to satisfy given criteria; for example recovering a very weak damping operator as the one proposed by Garnier [40] to prevent blow up in Generalized KdV equations in the supercritical case could be an interesting issue. Finally, the damping/stabilization technique presented here could be of interest when considering other dispersive equations such as those of Nonlinear Schrödinger Equation type, e.g. taking advantage of the works [37, 46].

Acknowledgments. The author would like to thank the two anonymous referees for their careful reading and valuable remarks.

REFERENCES

[1] H. Abboud, C. Al Kosseifi and J.-P. Chehab, A stabilized bi-grid method for Allen-Cahn equation in finite elements, *Comput. Appl. Math.*, **38** (2019), Paper No. 35, 27 pp.

[2] M. Abounouh, H. Al Moatassime, J-P. Chehab, S. Dumont and O. Goubet, Discrete Schrödinger equations and dissipative dynamical systems, *Commun. Pure Appl. Anal.*, **7** (2008), 211–227.

[3] K. Adamy, A. Bousquet, S. Faure, J. Laminie and R. Temam, A multilevel method for finite volume discretization of the two-dimensional nonlinear Shallow-Water equations, *Ocean Modelling,* **33** (2010), 235–256.

[4] R. E. Bank, Hierarchical bases and the finite element method, *(English) Iserles, A. (ed.), Acta Numerica*, Vol. 5, 1996. Cambridge: Cambridge University Press. (1996), 1–43.

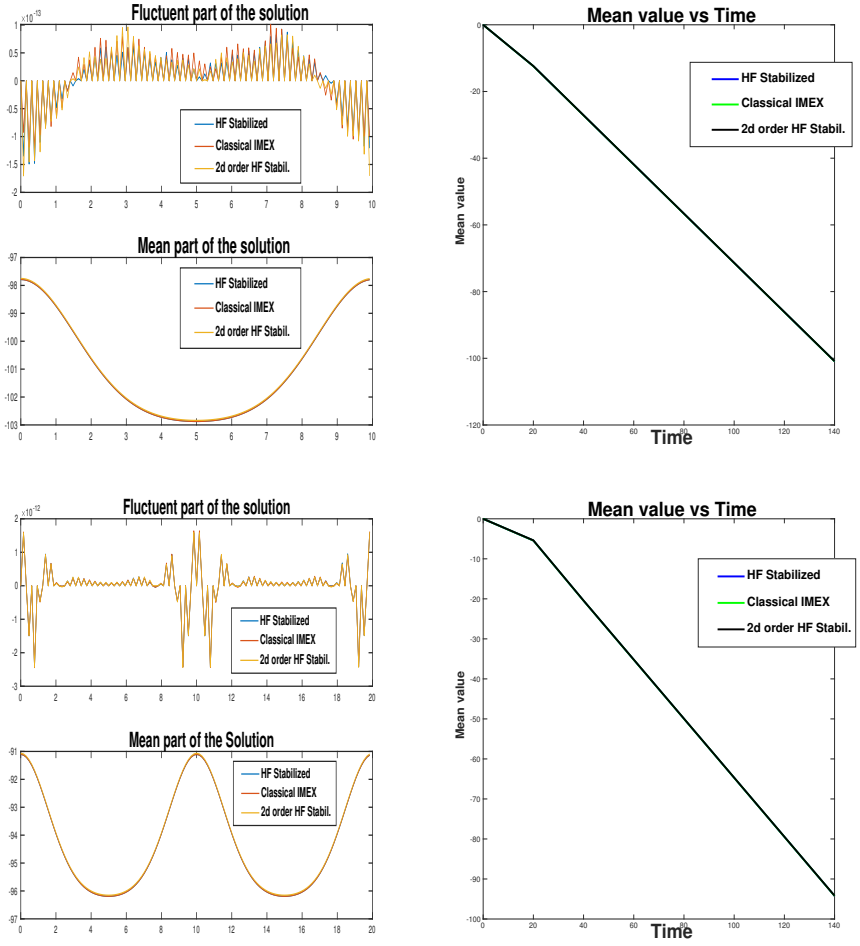

FIGURE 17. KSE Low and high frequency components of the solution at final time $T = 140$ (left), time evolution of the mean value (right) - $n = 128,\ m = 8,\ \Delta t = 0.01,\ L = 10$ (line 1), $L = 20$ (line 2)

[5] J. Bona and R. Smith, Existence of solutions to the Korteweg-de Vries initial value problem, In *Nonlinear Wave Motion* (Proc. AMS-SIAM Summer Sem., Clarkson Coll. Tech., Potsdam, N.Y., 1972), Lectures in Appl. Math., Amer. Math. Soc., Providence, R.I., **15** (1974), 179–180.

[6] J. L. Bona, M. Chen and J.-C. Saut, Boussinesq equations and other systems for small amplitude long waves in nonlinear dispersive media: II. the nonlinear theory, *Nonlinearity*, **17** (2004), 925–952.

[7] J. L. Bona and R. Smith, The initial-value problem for the Korteweg-de Vries equation, *Philos. Trans. Roy. Soc. London Ser. A*, **278** (1975), 555–601.

[8] M. Brachet and J.-P. Chehab, Stabilized times schemes for high accurate finite differences solutions of nonlinear parabolic equations, *J. Sci. Comput.*, **69** (2016), 946–982.

[9] M. Brachet and J.-P. Chehab, Fast and stable schemes for phase fields models, *Comput. Math. Appl.*, **80** (2020), 1683–1713.

[10] M. Brachet, *Schémas Compacts Hermitiens sur la sphère - Applications en Climatologie et Océanographie Numérique*, Thèse, Université de Lorraine, Jully 2018 (in French).

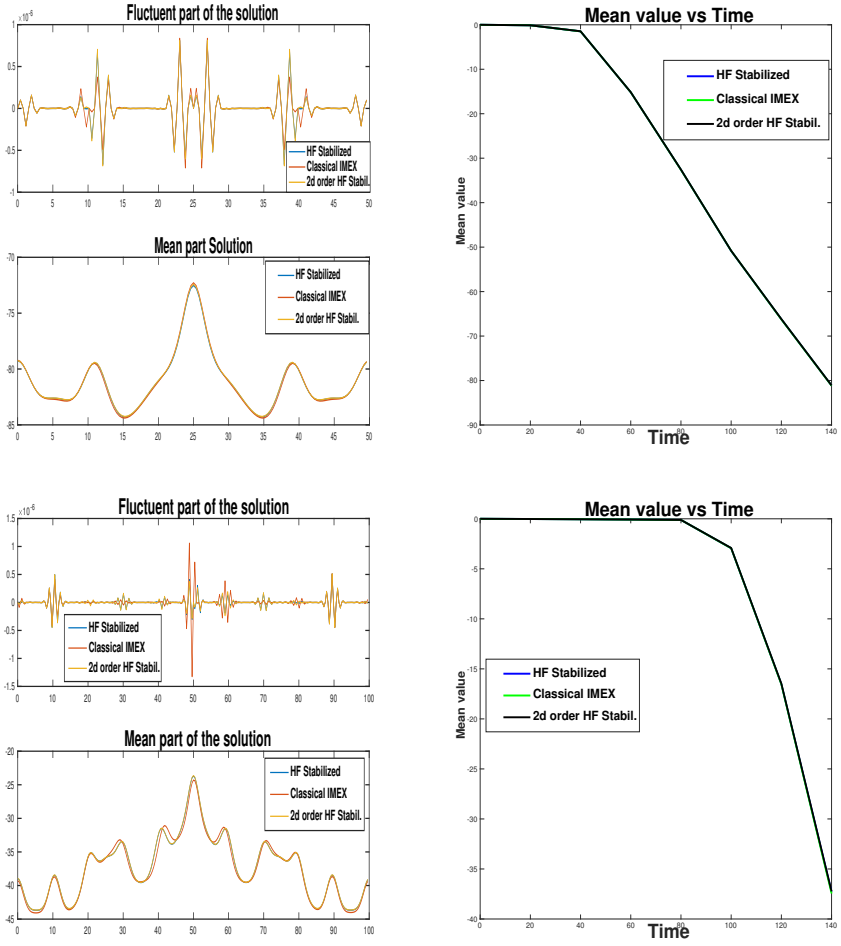

FIGURE 18. KSE Low and high frequency components of the solution at final time $T = 140$ (left), time evolution of the mean value (right) - $\Delta t = 0.01$. Line 1: $L = 50$, $n = 128$, $m = 8$; line 2: $L = 100$, $n = 256$, $m = 10$

[11] C. Brezinski and J.-P. Chehab, Nonlinear hybrid procedures and fixed point iterations, *Numer. Funct. Anal. Optim.*, **19** (1998), 465–487.

[12] M. Cabral and R. Rosa, Chaos for a damped and forced KdV equation, *Phys. D*, **192** (2004), 265–278.

[13] C. Calgaro, J.-P. Chehab, J. Laminie and E. Zahrouni, Séparation des échelles et schémas multiniveaux pour les équations d'ondes non-linéaires, (French) [Scale separation and multilevel schemes for nonlinear wave equations] CANUM, (2008), 180–208, *ESAIM Proc.*, 27, EDP Sci., Les Ulis, 2009.

[14] C. Calgaro, A. Debussche and J. Laminie, On a multilevel approach for the two-dimensional Navier-Stokes equations with finite elements, *Finite Elements in Fluids. Internat. J. Numer. Methods Fluids*, **27** (1998), 241–258.

[15] C. Calgaro, J. Laminie and R. Temam, Dynamical multilevel schemes for the solution of evolution equations by hierarchical finite element discretization, *Appl. Numer. Math.*, **23** (1997), 403–442.

[16] J.-P. Chehab and B. Costa, Multiparameter methods for evolutionary equations, *Numerical Algorithms*, **34** (2003), 245–257.
[17] J.-P. Chehab and B. Costa, *Multiparameter Extensions of Iterative Processes Rapport Technique du Laboratoire de Mathmatiques d'Orsay*, 2002.
[18] J.-P. Chehab and B. Costa, Time explicit schemes and spatial finite differences splittings, *J. Sci. Comput.*, **20** (2004), 159–189.
[19] J.-P. Chehab, P. Garnier and Y. Mammeri, Long-time behavior of solutions of a BBM equation with generalized damping, *Discrete Contin. Dyn. Syst. Ser. B*, **20** (2015), 1897–1915.
[20] J.-P. Chehab, P. Garnier and Y. Mammeri, Numerical solution of the generalized Kadomtsev-Petviashvili equations with compact finite difference schemes, submitted.
[21] J.-P. Chehab and G. Sadaka, Numerical study of a family of dissipative KdV equations, *Commun. Pure Appl. Anal.*, **12** (2013), 519–546.
[22] J.-P. Chehab and G. Sadaka, On damping rates of dissipative KdV equations, *Discrete Contin. Dyn. Syst. Ser. S*, **6** (2013), 1487–1506.
[23] M. Chen, S. Dumont, L. Dupaigne and O. Goubet, Decay of solutions to a water wave model with nonlocal viscous dispersive term, *Discrete Contin. Dyn. Syst.*, **27** (2010), 1473–1492.
[24] A. Cohen, *Numerical Analysis of Wavelet Methods*, North-Holland Publishing Co., Amsterdam, 2003.
[25] B. Costa, L. Dettori, D. Gottlieb and R. Temam. Time marching techniques for the nonlinear Galerkin method, *SIAM J. SC. Comp.*, **23** (2001), 46–65.
[26] A. Debussche, J. Laminie and E. Zahrouni, A dynamical multi-level scheme for the Burgers equation: Wavelet and hierarchical finite element, *J. Sci. Comput.*, **25** (2005), 445–497.
[27] T. Dubois, F. Jauberteau and R. Temam. *Dynamic Multilevel Methods and the Numerical Simulation of Turbulence*. Cambridge University Press, Cambridge, 1999.
[28] T. Dubois, F. Jauberteau and R. Temam, Incremental unknowns, multilevel methods and the numerical simulation of turbulence, *Comput. Methods Appl. Mech. Engrg.*, **159** (1998), 123–189.
[29] S. Dumont and J.-B. Duval, Numerical investigation of asymptotical properties of solutions to models for water waves with non local viscosity, *Int. J. Numer. Anal. Model.*, **10** (2013), 333–349.
[30] S. Dumont and I. Manoubi, Numerical analysis of a water wave model with a nonlocal viscous dispersive term using the diffusive approach, *Math. Methods Appl. Sci.*, **41** (2018), 4810–4826.
[31] D. Dutykh, Viscous-potential free-surface flows and long wave modelling, *Eur. J. Mech. B Fluids*, **28** (2009), 430–443.
[32] D. Dutykh and F. Dias, Viscous potentiel free-surface flows in a fluid layer of finite depth, *C. R. Math. Acad. Sci. Paris*, **345** (2007), 113–118.
[33] H. Emmerich, *The Diffuse Interface Approach in Materials Science Thermodynamic*, Concepts and Applications of Phase-Field Models. Lecture Notes in Physics Monographs, Springer, Heidelberg, 2003.
[34] A. Ern, J.-L. Guermond, *Theory and Practice of Finite Elements*, Applied Mathematical Science, 159, Springer-Verlag, New-York, 2004.
[35] D. J. Eyre, Unconditionallly Stable One-step Scheme for Gradient Systems, June 1998, unpublished, `http://www.math.utah.edu/eyre/research/methods/stable.ps`.
[36] E. Ezzoug, O. Goubet and E. Zahrouni, Semi-discrete weakly damped nonlinear 2-D Schrödinger equation, *Differential Integral Equations*, **23** (2010), 237–252.
[37] S. Faure, J. Laminie and R. Temam, Finite volume discretization and multilevel methods in flow problems, *J. Sci. Comput.*, **25** (2005), 231–261.
[38] *FreeFem++ Page*, `http://www.freefem.org`
[39] P. Garnier, Damping to prevent the blow-up of the Korteweg-de Vries equation, *Commun. Pure Appl. Anal.*, **16** (2017), 1455–1470.
[40] S. Gasparin, J. Berger, D. Dutykh and N. Mendes, Stable explicit schemes for simulation of nonlinear moisture transfer in porous materials, *J. Build. Perf. Sim.*, **11** (2017), 129–144.
[41] J.-M. Ghidaglia, Weakly damped forced Korteweg-de Vries equations behave as a finite dimensional dynamical system in the long time, *J. Differential Equations*, **74** (1988), 369–390.
[42] J.-M. Ghidaglia, A note on the strong convergence towards attractors for damped forced KdV equations, *J. Differential Equations*, **110** (1994), 356–359.
[43] O. Goubet, Asymptotic smoothing effect for weakly damped forced Korteweg-de Vries equations, *Discrete Contin. Dynam. Systems*, **6** (2000), 625–644.

[44] O. Goubet and R. M. S. Rosa, Asymptotic smoothing and the global attractor of a weakly damped KdV equation on the real line, *J. Differential Equations*, **185** (2002), 25–53.
[45] O. Goubet and E. Zahrouni, On a time discretization of a weakly damped forced nonlinear Schrödinger equation, *Commun. Pure Appl. Anal.*, **7** (2008), 1429–1442.
[46] J. M. Hyman and B. Nikolaenko, The Kuramoto-Sivashinky equation: A bridge between PDE's and dynamical systems, *Physica D*, **18** (1986), 113–126.
[47] M. S. Jolly, R. Rosa and R. Temam, Accurate computations on inertial manifolds, *SIAM J. Sci. Comput.*, **22** (2000), 2216–2238.
[48] C. Klein and R. Peter, Numerical study of blow-up and dispersive shocks in solutions to generalized Korteweg-de Vries equations, *Phys. D*, **304/305** (2015), 52–78.
[49] C. Laurent, L. Rosier and B.-Y. Zhang, Control stabilization of the Korterweg-de Vries equation in a periodic domain, *Comm. Partial Differential Equations*, **35** (2010), 707–744.
[50] S. K. Lele, Compact difference schemes with spectral-like resolution, *J. Comp. Phys.*, **103** (1992), 16–42.
[51] C. Lemaréchal, Une méthode de résolution de certains systèmes non linéaires bien posés, *C. R. Acad. Sci. Paris, sér. A*, **272** (1971), 605–607.
[52] M. Marion and R. Temam, Nonlinear Galerkin methods, *SIAM J. Numer. Anal.*, **26** (1989), 1139–1157.
[53] M. Marion and R. Temam, Nonlinear Galerkin methods: The finite elements case, *Numer. Math.*, **57** (1990), 205–226.
[54] M. Marion and J. Xu, Error estimates on a new nonlinear Galerkin method based on two-grid finite elements, *SIAM J. Numer. Anal.*, **32** (1995), 1170–1184.
[55] N. Mendes, M. Chhay, J. Berger and D. Dutykh, Explicit schemes with improved CFL condition, *Numerical Methods for Diffusion Phenomena in Building Physics*, (2020), 103–120.
[56] E. Ott and R. N. Sudan, Nonlinear theory of ion acoustic wave with Landau damping, *Phys. Fluids*, **12** (1969), 2388–2394.
[57] E. Ott and R. N. Sudan, Damping of solitary waves, *Phys. Fluids*, **13** (1970), 1432–1435.
[58] A. F. Pazoto and L. Rosier, Uniform stabilization in weighted Sobolev spaces for the KdV equation posed on the half-line, *Discrete Contin. Dyn. Syst. Ser. B*, **14** (2010), 1511–1535.
[59] P. Poullet, Staggered incremental unknowns for solving Stokes and generalized Stokes problems, *Appl. Numer. Math.*, **35** (2000), 23–41.
[60] J. Shen, Efficient Spectral-Galerkin method I. Direct solvers for the second and fourth order equations using legendre polynomials, *SIAM J. Sci. Comput.*, **15** (1994), 1489–1505.
[61] J. Shen, Efficient spectral-Galerkin method II. Direct solvers of second and fourth order equations using Chebyshev polynomials, *SIAM J. Sci. Comput.*, **16** (1995), 74–87.
[62] J. Shen and X. Yang, Numerical approximations of Allen-Cahn and Cahn-Hilliard equations, *Discrete Contin. Dyn. Syst.*, **28** (2010), 1669–1691.
[63] R. Temam, *Infinite Dimensional Dynamical Systems in Mechanics and Physics*, Applied Mathematical Science, Springer Verlag, 68, 1997, second augmented version.
[64] R. Temam and A. Miranville, *Mathematical Modeling in Continuum Mechanics,* Second edition, Cambridge University Press, Cambridge, 2005.
[65] H. Yserentant, On multilevel splitting of finite element spaces, *Numer. Math.*, **49** (1986), 379–412.
[66] L.-B. Zhang, *Un Schéma de Semi-Discrétisation en Temps Pour des Systèmes Différentiels Discrétisés en Espace Par la Méthode de Fourier. Résolution Numérique des Équations de Navier-Stokes Stationnaires Par la Méthode Multigrille*, PhD Thesis, Université Paris Sud, 1987.

Received June 2020; revised December 2020.

E-mail address: Jean-Paul.Chehab@u-picardie.fr